C.2

SEDIMENTATION BETWEEN PARALLEL PLATES

By

Yonas Kinfu Paulos

B. E., Anna University

A THESIS SUBMITTED IN PARTIAL FULFILLMENT OF

THE REQUIREMENTS FOR THE DEGREE OF

MASTERS OF APPLIED SCIENCE

in

THE FACULTY OF GRADUATE STUDIES

CIVIL ENGINEERING

We accept this thesis as conforming

to the required standard

THE UNIVERSITY OF BRITISH COLUMBIA

April 1991

In presenting this thesis in partial fulfilment of the requirements for an advanced degree at the University of British Columbia, I agree that the Library shall make it freely available for reference and study. I further agree that permission for extensive copying of this thesis for scholarly purposes may be granted by the head of my department or by his or her representatives. It is understood that copying or publication of this thesis for financial gain shall not be allowed without my written permission.

Department of CIVIL ENGINEERING

The University of British Columbia
Vancouver, Canada

Date May-03-1991

Abstract

Settling basins can be shortened by using a stack of horizontal parallel plates which develop boundary layers in which sedimentation can occur. The purpose of this study is to examine the design parameters for such a system and to apply this approach to a fish rearing channel in which settling length is strictly limited.

Flow between parallel rough and smooth plates has been modelled together with sediment concentration profile. Accurate description of boundary layer flow requires the solution of Navier-Stokes equations, and due to the complexity of the equations to be solved for turbulent flow some assumptions are made to relate the Reynolds stresses to turbulent kinetic energy and turbulent energy dissipation rate. The simplified equations are solved using a numerical method which uses the approach given by the TEACH code. The flow parameters obtained from the turbulent flow model are used to obtain the sediment concentration profile within the settling plates. Numerical solution of the sedimentation process is obtained by adopting the general transport equation. The lower plate is assumed to retain sediments reaching the bottom.

The design of a sedimentation tank for a fish rearing unit with high velocity of flow has been investigated. The effectiveness of the sedimentation tank depends on the uniformity of flow attained at the inlet, and experiments were conducted to obtain the most suitable geometric system to achieve uniform flow distribution without affecting other performances of the fish rearing unit. The main difficulties to overcome were the heavy circulation present in the sedimentation tank and the clogging of the distributing system by suspended particles. Several distributing systems were investigated, the best is discussed in detail.

It was concluded that a stack of horizontal parallel plates can be used in fish rearing systems where space is limited for settling sediments. Flow distribution along the vertical at the entrance to the plates determines the efficiency of the sediment settling process and a suitable geometrical configuration can be constructed to distribute the high velocity flow uniformly across the vertical. Numerical modelling of sediment removal ratio for flow between smooth and rough parallel plates has been calculated. The results show that almost the same pattern of sediment deposition occurs for both the smooth-smooth and rough-smooth plate arrangements.

Table of Contents

List of Tables

List of Figures

List of Symbols

a	- coefficient
a_y	- acceleration in y direction
A	- deposition coefficient, or area
A_p	- projected surface area
b	- width of flow
c	- sediment concentration, instantaneous
$\overline{c}$	- concentration, average
c'	- concentration, fluctuating
C	- concentration or drag coefficient
C_1	- a constant
C_2	- a constant
C_D	- drag coefficient
C_μ	- a constant
d	- diameter of particle
D	- drag force or diameter
E, E_1	- constants
f	- weighting factor for momentum flux
F	- flux
Fr	- Froude number
g	- acceleration due to gravity
g_1	- sediment transport per unit area
G	- turbulence generation term

H - depth of flow

i, j, k - coordinate directions

k - kinetic energy per unit mass, turbulent

k_s - roughness size

K_s^+ - roughness size, non-dimensional

l - mixing length

L - length of basin

L_1 - length of basin for half sediment deposition

n, s, e, w - direction notation, for faces

N, S, E, W - direction notation, for nodes

p - pressure

P_e - Peclet number

Q - flow discharge

r - removal ratio of sediment

R_ϕ - residual

$\Re$ - Reynold's number

S - slope

t - time

S_p - source term

S_s - specific gravity of particle

S_ϕ - a general source term

U - local horizontal velocity of flow

U_0 - average horizontal velocity

U_{max} - maximum local horizontal velocity of flow

U_τ - shear velocity

U^+ - velocity, non-dimensional

V - local vertical velocity of flow

$\hat{V}$ - characteristic velocity

V_s - mean settling velocity of suspension

V_s' - fall velocity correction value

V_{so} - overflow rate

VOL - elemental volume

x - horizontal axis coordinate

y - vertical axis coordinate from bed

y^+ - grid distance, non-dimensional

α - a coefficient

β - correlation coefficient or a coefficient

Γ - diffusion coefficient

δ - kronecker delta, boundary layer thickness

ϵ - energy dissipation

ϵ_m - transfer coefficient, momentum

ϵ_s - transfer coefficient, sediment

κ - von Karman constant

λ - time scale

μ - viscosity of fluid, laminar

μ_{eff} - viscosity of fluid, effective

μ_t - viscosity of fluid, turbulent

ν - kinematic viscosity of fluid, laminar

ρ - density of fluid

ρ_s - density of particle

σ_y - std. dev. for sediment trajectory

τ - shear stress

τ_w - shear stress at wall

ϕ - quantity to be transported

Acknowledgement

I am deeply grateful to Dr. Michael C. Quick for his unfailing support , encouragement and patience throughout the study. Without his advice and understanding this project would not have been possible. I would like to thank also Mr. Jeffery Quick for his help in computational flow modelling and Mr. Kurt Neilsen for his constant help in the laboratory work.

I am thankful to CIDA and Water Resources Commission (Ethiopia) for the financial support provided. Discussions and cooperation with Mr. Jim Bomford of the B.C. Department of the Environment, Fisheries Branch with regard to the work done on the flow distributing system are gratefully acknowledged.

Finally I praise God for giving me the strength to finish this project and also for making all things happen.

Chapter 1

INTRODUCTION

Water is a basic necessity for the existence of man, and as a resource it is found in different quantities and qualities. The required quantity and quality for consumption depends on the type of utilization, and it is the task of water engineering to provide the required demand reasonably and economically.

Sediments in water for use with hydro-electric power plant cause turbine blade abrasion to complete damage. In irrigation canals deposited sediments facilitate growth of weed, which increases the flow resistance and hence reduces the carrying capacity of a canal. One major problem is the removal of sediment from flowing water, especially at canal intakes, at hydro electric installations and water intakes. A special situation is removal and control of sediments for fish rearing systems and the present study was initiated to examine a particular type of fish rearing system. However, the sediment control techniques and the basic computational method and experiments can have wide application to other types of sediment control.

Rivers are the major sources of water supply. But often they are loaded with fine and coarse sediments. Different methods are used to reject and divert the sediments at intakes, but still fine sediments find their way into canals. Sedimentation basins are employed to remove fine sediments. Classical sedimentation basins facilitate sedimentation process by providing low and uniform velocity with low level of turbulence.

The study presented in this paper was initiated from the need to design a suitable sedimentation tank for a fish rearing system. The problem dealt with is different from the

classical type of sedimentation basins and the proposed sedimentation tank uses a stack of horizontal parallel plates for efficient use of space. Also the fish rearing channel has to be separated from the sedimentation tank so that sediments can be removed without interfering with the young fish. In addition, it is desired to design the system so that the water level can be kept constant. These constraints lead to complications in the design of the inlet flow to the settling tank so that the flow entering the settling tank tends to have a high velocity and a non-uniform distribution. This high velocity flow from the rearing unit also creates a circulation which has to be overcome by designing a suitable system. Therefore the task has been to have uniform distribution of flow in the settling tank without circulation and to study ways of increasing the efficiency of settling within the parallel plates.

For a turbulent flow there exists a velocity fluctuation in the vertical direction near a horizontal solid boundary. Bagnold('66) based on photographs taken by Prandtl('55) suggests that the upward and downward velocity fluctuations are unequal in magnitude, that is, the turbulence is unsymmetrical. Hence, this inequality in velocity fluctuation induces a net upward stress which is responsible for supporting solid particles in suspension. If an unsymmetrical turbulence produced at the bed could create upward pressure, then in line with the same thinking, an unsymmetrical turbulence created at a top boundary of the flow surface would induce a downward pressure to push the sediments downwards. This reduces the amount of sediment that can be suspended in a flow.

The above argument is to be investigated as a way of increasing the sediment removal efficiency of a sedimentation basin. Experimental and numerical investigations are presented to study the effect on sedimentation of smooth and rough boundaries at top surface of flow.

A necessary theoretical background for the study is given in Chapter 2. A review of the different sedimentation methods that are used in different fields of application are

discussed in Chapter 3, with details given for high rate settlers. Based on the practical problem posed, Chapter 4 discusses the design and modelling of sedimentation tank for fisheries. Chapter 5 describes the development of theory for maximizing the sedimentation between parallel plates. The numerical modelling of flow and sedimentation for different kinds of flow are given in Chapter 6. Experimental methods and procedure used for the different types of flow selected are discussed in Chapter 7, and Chapter 8 describes the experimental and numerical results with discussions. Finally Chapter 9 concludes the whole study.

Chapter 2

THEORETICAL BACKGROUND

2.1 Fall Velocity

In the study of sediment transport and sedimentation the fall velocity of a particle is an important parameter describing the particle in relation to the fluid.

Depending on the concentration and type of particles encountered, four types of settling can occur: discrete particle, flocculation, hindered and compression. The latter three are commonly important for wastewater treatment. Discrete settling is the major phenomenon which is of importance for this study and will be discussed in detail.

When particles fall in a fluid at rest, gravitational force causes particles to accelerate until the retarding resistance force from the fluid equals the gravitational force. When this equilibrium condition is reached, there is no acceleration, and hence a constant velocity is attained which is called terminal velocity.

For fluids in motion, the fall velocity of a particle in water at rest is to be used for the numerical computation to obtain the deposition pattern of particles under the effect of turbulence.

2.1.1 Factors affecting fall velocity

The fall velocity of a particle depends on many factors such as Reynold's number of a particle, shape, particle roughness, proximity of the boundary, concentration (including the gradient), the velocity of flow (particle rotation) and turbulence. In most practical

problems all the above mentioned factors may act in group or simultaneously.

Analysis of fall velocities of particles of regular shapes such as circular cylinder, ellipsoids, discs and isometric particles have been studied by many investigators. For irregular shapes Albertson studied the effects by defining shape factors. Heywood represented the shape effect by introducing volume coefficients. For practical use each method requires a knowledge of particles proportion.

Camp('46) considers the effect of turbulence as delaying the settling of particles. Paradoxically, Jobson et al.('70) report that the effective fall velocity in turbulent flow is increased, specially of coarse particles. Their finding is based on experimental results; by back calculating the fall velocity from governing suspended sediments mathematical equation.

2.1.2 Theoretical equations

Newton in his classical law of sedimentation equated the drag resistance force as follows

$$D = CA_p\rho\frac{v_s^2}{2} \tag{2.1}$$

where C is drag coefficient, D is drag force, A_p is projected area of a particle, ρ is density of fluid, and V_S fall velocity. Later on it was verified that C is not constant but a function of Reynold's number, therefore it is substituted by C_D.

$$D = C_D A_p\rho\frac{v_s^2}{2} \tag{2.2}$$

The Reynold's number of a particle falling in fluid is computed using the effective diameter as length scale, the fall velocity as velocity scale and using the viscosity of the fluid. For very low Reynold's number Re$<$ 0.1, the inertia forces may be neglected with the respect to the viscous forces. Stoke(Graf('71)) obtained an analytical solution of Navier-Stokes equations for drag resistance by ignoring inertia force (laminar case) for

spherical particles as

$$D = 3\pi d\mu v_s \tag{2.3}$$

where d is particle diameter and μ is fluid viscosity. Further assumptions made in the derivation are no slip condition between fluid and a particle, and particles fall in an infinite calm fluid. Hence equating Equations 2.2 and 2.3

$$C_D = \frac{24}{Re} \tag{2.4}$$

where Re= $\frac{v_s d}{\nu}$.

The gravitational force of a falling particle (spherical) is given by

$$\frac{\pi d^3}{6}(\rho_s - \rho)g \tag{2.5}$$

Equating the gravitational and drag resistance forces; since the terminal velocity is reached when no net force is exerted

$$v_s = \left[\frac{4}{3}\frac{g(S_s - 1)d}{C_D}\right]^{\frac{1}{2}} \tag{2.6}$$

for the case of Stokes solution,

$$v_s = \frac{g(\rho_s - \rho)d^2}{18\mu} \tag{2.7}$$

Oseen(Graf('71)) considered some of the inertia terms in Navier-Stokes equations and obtained

$$C_D = \frac{24}{Re}\left(1 + \frac{3}{16}Re\right) \tag{2.8}$$

Other more rigorous solution of Oseen type have been obtained by Olson, Goldstein, etc.(Graf ('71)) to extend the applicability of the theoretical solutions. But Graf et al.(Graf('71)) question their accuracy beyond Re= 2.

The method of solution applied by Prandtl(Graf('71)) to solve Navier-Stoke equations for boundary layer problems gave more insights to the formulation of drag coefficients. For

higher Re, solutions for C_D are given by many investigators. Proudman et al.(Graf('71)) suggested applying perturbation theory and matching of asymptotic solution to Navier-Stokes equations. Jensen used relaxation techniques to solve the Navier-Stokes equations for drag coefficient numerically at different Re. Fromm gave numerical solutions for drag coefficients for flow with obstacles in channel flow for high Re by considering the development of von Kármán vortex street.

2.1.3 Empirical and Semi-empirical formulations

To predict the fall velocity at higher and wide range of Re many investigators have suggested empirical equations. Olson(Graf('71)) related C_D and Re for Re< 100

$$C_D = \frac{24}{Re}\left(1 + \frac{3}{16}Re\right)^{\frac{1}{2}} \tag{2.9}$$

Schiller et al., Dallavalle and Langmuir et al.(Graf('71)) have given similar empirical expressions for C_D.

Rubey(Graf('71)) suggests the combination of stokes law and Newton's formulation to obtain a pseudo-theoretical equation of fall velocity for large and small particles. Hence the total drag force for a spherical particles is given by,

$$D = 3\pi d\mu v_s + \pi\frac{d^2}{4}\rho v_s^2 \tag{2.10}$$

which can also be expressed as,

$$D = \left(\frac{24}{Re}\right) A_p\rho\frac{v_s^2}{2} + (2)A_p\rho\frac{v_s^2}{2} \tag{2.11}$$

Therefore,

$$C_D = \frac{24}{Re} + 2 \tag{2.12}$$

For $Re > 50$ Rubey's formula is not in good agreement with experimental data obtained for spherical particles. But many investigators in various areas of research

have preferred the formula. Einstein used Rubey's formula in developing his sediment transport equation in open channel flow.

2.1.4 Experimental data for natural quartz grains

The above discussed methods for obtaining fall velocity are less applicable for natural grains. Most of the theoretical results are related to spherical or other regular shaped particles. Moreover at higher Reynold's number the agreement with experimental result is not good. Since most of the experiments were conducted in wind tunnel consideration has to be made to relate them with the fall of a particle in water. Even the most popular Rubey's formula doesn't give good result at very high Reynold's number.

Mamak has given a table listing the relationship between grain diameter and fall velocity. Even though Mamak(Graf('71)) hasn't specified the grain type and fluid property his result is verified experimentally by Graf et al.(Graf('71)) for quartz grain in water with temperature of $20°C$. For computing the fall velocity of sand grains considered in this study the plotting given by Vanoni('75), is used which gives the values for wide range of temperatures. The fall velocity of a particle in water at rest is considered for the numerical computation of sediment concentration.

2.2 Sediment Transfer Coefficient

The sediment transfer coefficient is approximately analogous to the momentum transfer coefficient or kinematic eddy viscosity that is found in the theory of the diffusion of momentum. Hinze('59) has indicated the approximate analogy between momentum and mass transfer.

For channel flow the differential equation for sediment suspension in its simplest form

is given by,

$$\epsilon_s \frac{dC}{dy} + V_s C = 0 \tag{2.13}$$

where C is sediment concentration, ϵ_s is sediment transfer coefficient, y is vertical distance from the bottom. The complete derivation of the sediment suspension model is given in the next section.

Rearranging Equation 2.13

$$\epsilon_s = -\frac{V_s C}{\frac{dC}{dy}} \tag{2.14}$$

From accurate point measurement of concentration a graph of C against y may be plotted to calculate ϵ_s at any point on the curve. The value of ϵ_s at a point is calculated by estimating the slope of the tangent of the concentration curve where ϵ_s is to be evaluated.

For free surface flow the sediment transfer coefficient is assumed to depend on the fall velocity, depth of flow and shear velocity at the channel bed.

Therefore,

$$\epsilon_s = f\left(\frac{y}{H}, \frac{V_s}{U_*}\right) \tag{2.15}$$

where U_* is shear velocity, H is depth of flow.

For wide channel neglecting the head loss difference between wall and bed , the shear velocity may be calculated as follows,

$$U_* = (gHS)^{1/2} \tag{2.16}$$

where S is slope of basin.

As given by von Kármán and Vanoni('46) ϵ_s is assumed to be proportional to the momentum transfer coefficient ϵ_m. The ratio between the two quantities is written as $\frac{\mu_{eff}}{\rho \epsilon_s} = S_c$, which is often referred as turbulent Schmidt number. Where μ_{eff} is effective viscosity of fluid which includes viscous and turbulent values.

For turbulent flow,

$$\tau = \rho \frac{dU}{dy} \tag{2.17}$$

where τ is shear stress and U is mean local velocity of flow. And for two dimensional flow,

$$\tau = \tau_w \left(1 - \frac{y}{H}\right) \tag{2.18}$$

where τ_w is shear stress at wall. Combining both of the above equations,

$$\epsilon_m = \frac{\tau_w \left(1 - \frac{y}{H}\right)}{\rho \frac{dU}{dy}} \tag{2.19}$$

but from von Kármán universal velocity defect law,

$$\frac{U - U_{max}}{U_*} = \frac{1}{\kappa} ln \frac{y}{H} \tag{2.20}$$

where U_{max} is maximum flow velocity, and κ is von Kármán constant. Since $U_* = \sqrt{\tau_w/\rho}$, substituting

$$\epsilon_s = S_c \epsilon_m = S_c U_* \kappa \frac{y}{H} (H - y) \tag{2.21}$$

$$\frac{\epsilon_s}{U_* H} = S_c \kappa \frac{y}{H} \left(1 - \frac{y}{H}\right) \tag{2.22}$$

S_C is a proportionality constant which may depend on particle size and other factors. The above model indicates that ϵ_S should be zero at bed and water surface, and maximum near the mid-depth.

Observation made of ϵ_s variation over the depth indicate contrary to the model given by von Kármán. The data given by Coleman('70) for open channel flow indicates that, two regions exist for the value of ϵ_s. In the lower region ϵ_s varies with distance from the bed. In the upper region ϵ_s has values close to maximum and is almost constant up to the water surface.

Jobson et al.('70) has identified the existence of lower and upper sediment transfer regions in open channel flow, and in accordance has indicated the following two equations,

$$\frac{\epsilon_s}{U_* H} = 0.985\kappa \left(1 - \frac{y}{H}\right) \frac{y}{H} + 37.6 \left(\frac{y}{H}\right)^3 \; for \; y/H < 0.1 \tag{2.23}$$

$$\frac{\epsilon_s}{U_* H} = 0.985\kappa \left(1 - \frac{y}{H}\right) \frac{y}{H} + .0515 \left(\frac{y}{H}\right)^3 \; for \; y/H > 0.1 \tag{2.24}$$

The above equations indicate that the value of $\frac{\epsilon_s}{U_* H}$ approaches zero near the water surface which is contrary to the data obtained by Coleman('70), otherwise for κ value of 0.38 the equations seem to be close to the data obtained.

According to Coleman('70), the value of $\frac{\epsilon_s}{U_* H}$ varies directly with V_s/U_* which indicates that ϵ_s varies directly with the settling velocity for a given H and U_*. Therefore keeping other variables constant the sediment transfer is large for coarser sediment particles.

The experimental results of Coleman('70) indicate that for open channel flow the sediment transfer coefficient increases with distance away from the bed. A maximum value is reached at about 1/5 to 1/3 of the water depth from the channel bed. At the water surface the sediment transfer coefficient does not reach zero, but has a finite value.

Different investigators have compared the values of momentum transfer coefficient with sediment transfer coefficient. The results given seem to be contradictory. But Jobson et al. approached the evaluation of sediment transfer coefficient by considering the mechanics of a sediment particle. Consequently they give the explanation for the different results obtained. They consider the vertical mixing of a sediment particle to occur due to semi-independent processes which are diffusion due to tangential components of turbulent fluctuations, and diffusion due to centrifugal force initiated from the curvature of fluid particle path lines. Both components are shown to be additive.

For fine sediment particles the tangential components of turbulent velocity fluctuations seems to be dominant, which is also true for all sediment particles in flows without

strong vortex activity. This component is approximately proportional to the momentum transfer coefficient and decreases with larger particle size. For coarse sediments with strong vortex flow, diffusion due to the curvature of the fluid particle path lines seems to be significant. The sediment transfer coefficient due to centrifugal acceleration is assumed to reach maximum in the zone of intense shear stress and increases with increasing particle size in the fine to medium range. It is also closely related to the behavior of the bed roughness specifically to those which give rise to flow separation.

The distribution of sediment transfer coefficient in closed channel flow is discussed by Ismail('52). The derivation of the momentum transfer coefficient using the von Kármán universal velocity defect law gives zero value at the center. Von Kármán has stated that in the central part of a pipe the similarity assumption is correct. Brooks and Berggren(Ismail('52)) have indicated that the momentum transfer coefficient at the center has to be constant according to the results of Sherwood and Woertz(Ismail('52)) or an error curve has to be assumed for ϵ_m. Nikurade(Ismail('52)) gave definite values for ϵ_m at the center of pipes in his experimental results.

For numerical computation it is necessary to be able to calculate the sediment transfer coefficient and the momentum transfer coefficient. The sediment transfer coefficient at the center of a closed channel may be computed once the sediment concentration profile is obtained. The experimental result indicate that for the middle third of the channel the sediment transfer coefficient is almost constant. Due to the proportionality between the two transfer coefficients, the results discussed for ϵ_s could also represent the form of ϵ_m. Numerical computation results of flow in closed channel indicate a finite value of momentum transfer coefficient at the center (described in Chapter 8). As shown for the sediment transfer coefficient, ϵ_m has almost constant value near the middle of a channel.

For numerical computation of a sediment concentration, it is therefore reasonable to assume that the sediment transfer coefficient to be the same as the momentum transfer

coefficient. The same assumption was made by Camp('46), Sarikaya('77), and Bechteler et al.('84). The evaluation of the momentum transfer coefficient is discussed in the explanation of fluid flow computation model in the next section 2.3.

2.3 Flow and Sedimentation Models

2.3.1 Turbulent Flow Model

Background

Accurate description of flow requires the use of the exact equations expressing the principle of conservation of momentum: the Navier-Stokes equations.

For incompressible flow the equations expressing the principle of conservation of mass and momentum in Cartesian tensor co-ordinates are,

$$\frac{\partial U_i}{\partial x_i} = 0 \tag{2.25}$$

and

$$\rho\frac{\partial U_i}{\partial t} + \rho\frac{\partial}{\partial x_j}(U_iU_j) = -\frac{\partial p}{\partial x} + \frac{\partial}{\partial xj}\left\{\mu\left(\frac{\partial U_i}{\partial x_j} + \frac{\partial U_j}{\partial x_i}\right)\right\} \tag{2.26}$$

where p is pressure.

The instantaneous variable velocity may be decomposed as follows,

$$U_i = \overline{U_i} + u_i \tag{2.27}$$

where is u_i fluctuating velocity. The overbar indicates time-averaged value.

The time-averaged value $\overline{U_i}$ is defined as follows,

$$\overline{U_i} = \frac{1}{\Delta t}\int_t^{t+\Delta t} U_i dt \tag{2.28}$$

The combination of the above expressions give the Reynolds equations. The expression produces six new unknowns, the turbulent or Reynolds stresses $-\rho\overline{u_iu_j}$ which arise

from the averaging of the non-linear convective terms. The Reynolds stresses represent diffusion of momentum by turbulent motion. Since the unknowns are more than the equations given, additional equations are required to have a closed solution to the problem. These additional equations may be provided by making certain assumptions to model the Reynolds stresses.

k-ϵ Turbulence Model

The k-ϵ model, Launder and Spaldling('74), which is to be used in this study requires the solutions of two additional transport equations: one for the turbulent kinetic energy, k, and the other for the turbulent kinetic energy dissipation rate, ϵ. There seems to be a good compromise between generality and cost of computation in using the model.

Reynolds stresses are additive to the viscous terms in laminar flow and have similar effect on the flow, hence it is said that they are caused by eddy viscosity. The main basis for the k-ϵ model is the eddy viscosity concept. The concept is expressed by an equation as follows,

$$-\rho\overline{u_i u_j} = \mu_t \left(\frac{\partial u_i}{\partial x_j} + \frac{\partial u_j}{\partial x_i} \right) - \frac{2}{3}\rho k \delta_{ij} \tag{2.29}$$

where μ_t is turbulent viscosity and k is given by,

$$k = \frac{1}{2}\left(\overline{u_1^2} + \overline{u_2^2} + \overline{u_3^2}\right) \tag{2.30}$$

and δ is the Kronecker delta.

The eddy or turbulent viscosity is determined in terms of definable quantities. First it is assumed that μ_t is proportional to a characteristic velocity $\hat{V}$; and length scale ℓ.

$$\mu_t \propto \hat{V}\ell \tag{2.31}$$

Taking $\sqrt{k}$ as physically meaningful scale characterizing the turbulent velocity fluctuations, the above equation gives the Kolmogorov-Prandtl relation,

$$\mu_t \propto \rho\sqrt{k}\ell \tag{2.32}$$

By dimensional analysis k and ℓ are related to turbulent kinetic energy dissipation rate ϵ, Rodi('84), as follows

$$\epsilon \propto \frac{k^{3/2}}{\ell} \tag{2.33}$$

combining Equation 2.32 and 2.33

$$\mu_t = C_\mu \rho k^2/\epsilon \tag{2.34}$$

where C_μ is a proportionality constant to be determined empirically.

The problem of solving the turbulent stresses has thus been reduced to determining k and ϵ. Transport equations for k and ϵ are as obtained by Launder and Spadling('74). Hence in the k-ϵ model the transport equations for k and ϵ are given by

$$\rho U_k \frac{\partial k}{\partial x_k} = \frac{\partial}{\partial x_k}\left(\frac{\mu_{eff}}{\sigma_k}\frac{\partial k}{\partial x_k}\right) + \mu_{eff}\left(\frac{\partial U_i}{\partial x_k} + \frac{\partial U_k}{\partial x_i}\right)\frac{\partial U_i}{\partial x_k} - \rho\epsilon \tag{2.35}$$

and

$$\rho U_k \frac{\partial \epsilon}{\partial x_k} = \frac{\partial}{\partial x_k}\left(\frac{\mu_{eff}}{\sigma_\epsilon}\frac{\partial \epsilon}{\partial x_k}\right) + C_1\mu_{eff}\frac{\epsilon}{k}\left(\frac{\partial U_i}{\partial x_k} + \frac{\partial U_k}{\partial x_i}\right)\frac{\partial U_i}{\partial x_k} - C_2\rho^2/k \tag{2.36}$$

where the empirical constants are given in Table 2.1.

The effective viscosity, μ_{eff}, is given as the sum of laminar and eddy viscosity.

$$\mu_{eff} = \mu + \mu_t \tag{2.37}$$

$$\mu_t = C_\mu \rho \frac{k^2}{\epsilon} \tag{2.38}$$

Table 2.1: The k-ϵ model empirical constants

C_μ	C_1	C_2	σ_k	σ_ϵ	κ
0.09	1.44	1.92	1.0	$\frac{\kappa^2}{(C_2-C_1)C_\mu^{1/2}}$	0.4187

The above derivations give the approximation of turbulent variables of a flow.

General Flow Equations

For steady two-dimensional flow the general equations to be solved are

continuity equation:

$$\frac{\partial U}{\partial x}+\frac{\partial V}{\partial y}=0 \tag{2.39}$$

x-momentum equation:

$$\rho\frac{\partial}{\partial x}(UU)+\rho\frac{\partial}{\partial y}(VU)=-\frac{\partial p}{\partial x}+2\frac{\partial}{\partial x}\left(\mu_{eff}\frac{\partial U}{\partial x}\right)+\frac{\partial}{\partial y}\left\{\mu_{eff}\left(\frac{\partial U}{\partial y}+\frac{\partial V}{\partial x}\right)\right\} \tag{2.40}$$

y-momentum equation

$$\rho\frac{\partial}{\partial x}(UV)+\rho\frac{\partial}{\partial y}(VV)=-\frac{\partial p}{\partial x}+2\frac{\partial}{\partial x}\left(\mu_{eff}\frac{\partial V}{\partial y}\right)+\frac{\partial}{\partial y}\left\{\mu_{eff}\left(\frac{\partial V}{\partial x}+\frac{\partial U}{\partial y}\right)\right\} \tag{2.41}$$

k-transport equation:

$$\rho\frac{\partial}{\partial x}(Uk)+\rho\frac{\partial}{\partial y}(Vk)=\frac{\partial}{\partial x}\left(\frac{\mu_{eff}}{\sigma_k}\frac{\partial k}{\partial x}\right)+\frac{\partial}{\partial y}\left(\frac{\mu_{eff}}{\sigma_k}\frac{\partial k}{\partial y}\right)+G-\rho\epsilon \tag{2.42}$$

ϵ-transport equation:

$$\rho\frac{\partial}{\partial x}(U\epsilon)+\rho\frac{\partial}{\partial y}(V\epsilon)=\frac{\partial}{\partial x}\left(\frac{\mu_{eff}}{\sigma_\epsilon}\frac{\partial \epsilon}{\partial x}\right)+\frac{\partial}{\partial y}\left(\frac{\mu_{eff}}{\sigma_\epsilon}\frac{\partial \epsilon}{\partial y}\right)+C_1\frac{\epsilon}{k}G-C_2\rho\frac{\epsilon^2}{k} \tag{2.43}$$

where G, is the turbulent energy generation given as

$$G=\mu_t\left\{2\left[\left(\frac{\partial U}{\partial x}\right)^2+\left(\frac{\partial U}{\partial y}\right)^2\right]+\left(\frac{\partial U}{\partial y}+\frac{\partial V}{\partial x}\right)^2\right\} \tag{2.44}$$

Table 2.2: Transported quantity Γ and S_ϕ values

Transported quantity	ϕ	Γ	S_ϕ
Mass	1	0	0
x-momentum	U	μ_{eff}	$-\frac{\partial p}{\partial x}+\frac{\partial}{\partial x}\left(\mu_{eff}\frac{\partial U}{\partial x}\right)+\frac{\partial}{\partial y}\left(\mu_{eff}\frac{\partial V}{\partial x}\right)$
y-momentum	V	μ_{eff}	$-\frac{\partial p}{\partial y}+\frac{\partial}{\partial x}\left(\mu_{eff}\frac{\partial U}{\partial y}\right)+\frac{\partial}{\partial y}\left(\mu_{eff}\frac{\partial V}{\partial y}\right)$
Tur. Kine. Energy	k	$\frac{\mu_{eff}}{\sigma_k}$	$G-\rho\epsilon$
Tur. Kine. Energy Dissp.	ϵ	$\frac{\mu_{eff}}{\sigma_\epsilon}$	$C_1\frac{\epsilon}{k}G-C_2\rho\frac{\epsilon^2}{k}$

For convenience of numerical purposes the Equations 2.39 to 2.44 may be represented by general transport equation

$$\rho\frac{\partial}{\partial x}(U\phi)+\rho\frac{\partial}{\partial y}(V\phi)=\frac{\partial}{\partial x}\left(\Gamma\frac{\partial\phi}{\partial x}\right)+\frac{\partial}{\partial y}\left(\Gamma\frac{\partial\phi}{\partial y}\right)+S_\phi \tag{2.45}$$

where ϕ is quantity to be transported, Γ is general diffusivity coefficient and S_ϕ a general source term. For each transported quantity; the particular values of Γ and S_ϕ are given in Table 2.2.

The general transport expression given by Equation 2.45 will be used for the numerical computation of each flow variables.

2.3.2 Sedimentation Model

Many theories have been forwarded to explain the process of sediment suspension in a turbulent fluid. Some of the theories are: 1) suspension of sediment occurs when the hydrodynamic lift force is greater than the submerged weight; 2) sediment is entrained due to turbulent fluctuation at the bed; 3) the loss of contact of a particle with the bed due to instability induced by irregularities on the bed; 4) due to the disruption of particles on the bed by eddies. All of the theories require turbulence in the fluid to produce suspension. The effect of turbulence in suspending sediment particles may be

derived in a similar way as the shear stress in a turbulent fluid.

Let a two-dimensional uniform turbulent flow with sediment particles of uniform size, shape, and density be considered. Let U be the mean horizontal velocity in x-direction, and y be the vertical axis. Since the flow is assumed uniform and two-dimensional, the concentration varies only in the vertical. Due to concentration variation in the vertical diffusion of sediment particles occurs. Let v be the fluctuating component of the vertical instantaneous velocity. At any instant the vertical fluid transported across elemental area of $dx\,dy$ is $v\,dx\,dy$. The instantaneous rate of transport of sediment in the vertical will be $v\,c\,dx\,dy$, where c is the instantaneous concentration. The transport of sediment per unit area is given by

$$g_1 = \overline{vc} \tag{2.46}$$

where $c = \bar{c} + \acute{c}$, $\bar{c}$ is average sediment concentration, and $\acute{c}$ is the fluctuating component. Combining Equations 2.45 and 2.46

$$g_1 = \overline{v(\bar{c} + \acute{c})} = \overline{v\bar{c}} + \overline{v\acute{c}} \tag{2.47}$$

but $\overline{v\bar{c}} = 0$ since there is no net transport of fluid in the vertical direction, $\bar{v} = 0$. Therefore, Equation 2.47 becomes

$$g_1 = \overline{v\acute{c}} \tag{2.48}$$

From the definition of v and $\acute{c}$ it is clear that they can vary in magnitude and sign at a particular instance. Therefore, the average of their product may not reduce to zero.

Sediment concentration decreases away from a bed due to gravitational force acting on the grains. Therefore any fluid moving upwards or downwards through section $dx\,dy$ will have come from a region with higher concentration. This indicates that v is associated

with $\acute{c}$ and $-v$ with $-\acute{c}$. Therefore the product $\overline{v\acute{c}}$ would be always positive contributing to the upwards movement of sediment.

Considering the general case that the value $\overline{\acute{c}v}$ is non-zero, $\acute{c}$ and v may be correlated. The degree of correlation may be expressed by a correlation coefficient, β, given by

$$\beta = \frac{\overline{\acute{c}v}}{\sqrt{\overline{\acute{c}^2}}\sqrt{\overline{v^2}}} \tag{2.49}$$

For convenience of formulating the above equation it may be assumed that

$$\sqrt{\overline{\acute{c}^2}} = l_1 \left|\frac{dc}{dy}\right| \tag{2.50}$$

where l_1 = length scale which can be considered as analogous with the fluid flow as mixing length, l, defined by Prandtl. Therefore substituting the assumed Equations 2.50 into Equation 2.49

$$g_1 = -|\beta|\sqrt{\overline{v}^2} l_1 \frac{d\bar{c}}{dy} \tag{2.51}$$

The minus sign is to indicate that transport of sediment is in the direction of decreasing concentration. It can be clearly shown from Fick's Law that in the above expression the product $|\beta|\sqrt{\overline{v}^2} l_1$ gives diffusion coefficient. Therefore

$$\epsilon_s = |\beta|\sqrt{\overline{v}^2} l_1 \tag{2.52}$$

and

$$g_1 = -\epsilon_s \frac{dC}{dy} \tag{2.53}$$

The above expression is similar to the shear stress derivation of turbulent two-dimensional flow.

In deriving Equation 2.53, it was assumed that the flow is steady, hence the average concentration at any level will be constant and the net average sediment flow through a horizontal is zero. Therefore, the upwards sediment diffusion due to turbulence is balanced by downwards movement of sediment due to gravitation which is represented by settling velocity. The settling rate per unit area due to gravity is given by CV_s. Equating the upward and downward transport of sediment for equilibrium condition

$$\epsilon_s \frac{dC}{dy} + CV_s = 0 \tag{2.54}$$

The above equation was first used by W. Schmidt(Vanoni('46)) in the study of suspension of dust particles in the atmosphere, and by M.P. O'Brien(Vanoni('46)) in the study of suspended sediments in streams.

The flow in sedimentation basins may be treated as a stream flow with sediments. But the above derivation assumes that the horizontal velocity and sediment concentration along the flow direction is uniform. Therefore to study the sedimentation process in a developing flow, with boundary layer development, a more general mathematical expression is required.

Let an elemental volume with unit width and $\Delta x \Delta y$ area be considered. In time Δt, the flow of sediment into the elemental volume less the flow sediment out of the elemental volume equals the change of concentration in the volume. The net upward transport of sediment is represented by $\epsilon_s \partial C/\partial y$. The sediment transfer coefficient in the x-direction is taken to be equal with the sediment transfer coefficient in the y-direction, ϵ_s. Therefore, transport of sediment in the horizontal direction is given by $\epsilon_s \partial C/\partial x$. In many cases this term is omitted since the concentration gradient along the horizontal is very low. The downward transport of sediment due to the weight of the grains is given by CV_s. The various terms involved with respect to the elemental volume are show in Figure 2.1.

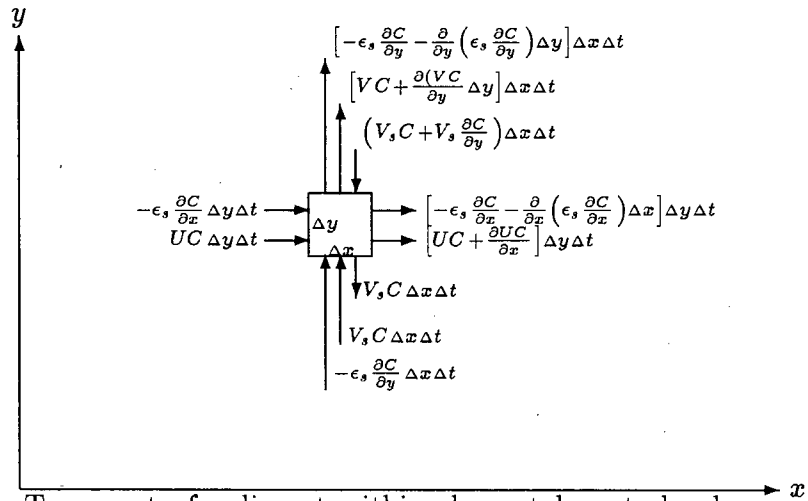

Figure 2.1: Transport of sediment within elemental control volume

Equating the inflow and outflow with change in concentration

$$\frac{\partial C}{\partial t}\Delta x \Delta y \Delta t = \left[-\frac{\partial}{\partial x}(UC) + \frac{\partial}{\partial x}\left(\epsilon_s \frac{\partial C}{\partial x}\right) - \frac{\partial}{\partial x}(VC) + \frac{\partial}{\partial y}\left(\epsilon_s \frac{\partial C}{\partial y}\right) + V_s \frac{\partial C}{\partial y}\right]\Delta x \Delta y \Delta t \tag{2.55}$$

Dividing by $\Delta x\,\Delta y\,\Delta t$ the above equation, and considering a steady state condition, $\partial C/\partial t = 0$, gives

$$\frac{\partial (UC)}{\partial x} + \frac{\partial (VC)}{\partial y} = \frac{\partial}{\partial x}\left(\epsilon_s \frac{\partial C}{\partial x}\right) + \frac{\partial}{\partial y}\left(\epsilon_s \frac{\partial C}{\partial y}\right) + V_S \frac{\partial C}{\partial y} \tag{2.56}$$

The above equation matches with the formulation of the general transport equation given by Equation 2.45. The equivalent values are given in Table 2.3. In deriving the above equation only the kinematics of the flow is considered. The dynamic effect of sediment is to be considered in fluid flow formulation. It has been shown by Vanoni('46) that the von kármán constant κ changes with sediment concentration level. The change in

Table 2.3: Sedimentation Model Γ and S_ϕ values

	ϕ	Γ	S_ϕ
Sediment Concentration	C	$\rho\epsilon_s$	$V_s\frac{\partial C}{\partial y}$

κ has an effect on the profile of velocity distribution. Bechteler et al.('84) have indicated that a sedimentation process is not influenced significantly for $0.28 < \kappa < 0.44$.

At the top surface of the flow, whether there be boundary or not the net transport of sediment in the vertical has to be zero. Expressing it mathematically

$$\epsilon_s\frac{\partial C}{\partial y} + V_s C = 0 \qquad at \quad y = H \tag{2.57}$$

For higher efficiency of sedimentation basins, resuspension or scouring of sediments is to be avoided. Therefore, it is assumed that sediments reaching the bottom or bed are removed from the flow completely. The general boundary condition for the bed is given by

$$\epsilon_s\frac{\partial C}{\partial y} + (1-A)V_s C = 0 \qquad at \quad y = 0 \tag{2.58}$$

where A is defined by Çecen et al.('71) as bed-absorbency coefficient. It represents the probability that a particle reaching the bed is deposited. For sedimentation basins with no resuspension the value is taken as unity.

Chapter 3

PREVIOUS WORK ON SEDIMENTATION METHODS

Many types of sedimentation basins are available for practical applications. The selection depends on the type of suspension to be removed, size of suspended particles, flow volume, relative cost and practical constraints or design features related with other structures.

In this chapter the basic features of many related sedimentation methods are discussed with brief introduction of the ideal sedimentation theory.

Ideal Basin

For design purposes, the classical theory of sedimentation was first given by Hazen('04). He showed that the removal ratio of suspended matter depends on the surface area provided and not upon the detention period or volume of basin and his argument is outlined below. The ideal rectangular continuous flow basin for unhindered quiescent discrete settling assumes the following

- horizontal, steady and uniform velocity of flow

- the concentration of each size particle is the same along the vertical at the inlet

- solid particle is removed from suspension once it reaches the bed

The removal ratio of suspended matter is one minus the ratio between outlet to inlet concentration of sediment. The detention period is defined as time required for suspension to reach bottom of basin.

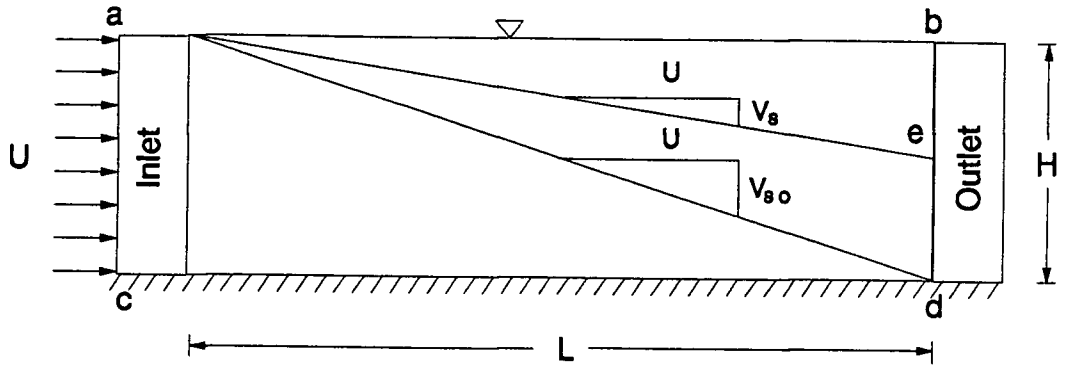

Figure 3.1: Ideal rectangular sedimentation basin

The formulation of ideal sedimentation tank is given by Fig. 3.2. The removal ratio of suspension, r, from similarity of triangles

$$r = \frac{\overline{be}}{\overline{ed}} = \frac{V_s}{V_{so}} \tag{3.1}$$

where V_s is the settling velocity, V_{so} is the overflow rate defined as the flow rate divided by plan area considered of a basin.

The overflow rate at length L from the inlet is given by

$$V_{so} = \frac{Q}{BL} \tag{3.2}$$

where Q is the volume flow rate, and B the width of basin. Therefore combining Eq. 3.1 and Eq. 3.2

$$r = \frac{BLV_s}{Q} \tag{3.3}$$

which indicates that the removal ratio for a given discharge and suspension (or mean settling velocity) depends on BL which is the surface area of the basin.

The above analysis doesn't include the effects of turbulence, resuspension, inlet and outlet conditions on sedimentation process. The theory is based on the idea of "overflow rate"

3.1 High-rate Settlers

3.1.1 Introduction

It is clearly seen from the ideal basin theory that the surface area of a basin is important design feature. For discrete settling without turbulence, the depth within wide range is not important design parameter except for other practical constraints.

High-rate settlers employ a set of parallel plates or pipes arranged horizontally or inclined with detention period not longer than 15 min. Within a limited plan area a multiple settling area is provided. This reduces the cost of construction and the use of land for building a basin. The increased surface area increases resistance, which lowers the Reynold's number of the flow, and under these circumstances, turbulence is reduced so that particle settling is increased. The high rate settlers are mainly used in water and wastewater treatments.

3.1.2 Different Types of High-rate Settlers

Three distinct types of high-rate settlers may be identified. Tube settlers consist of tubes of various cross-sections, such as hexagonal rectangular or circular. The steeply inclined tube settlers , have an inclination between 45° and 60° to self-cleanse the sludge deposited at the wall of tubes. The other type of tube settler which is essentially horizontal at inclination of 5°. The small inclination facilitates the flushing of sludge by backwashing. The setup of tube settlers is given by Fig. 3.2. A typical dimension of the settlers may be about $750mm$ of length and $50mm$ of across flats of tube. For inclined tube settlers

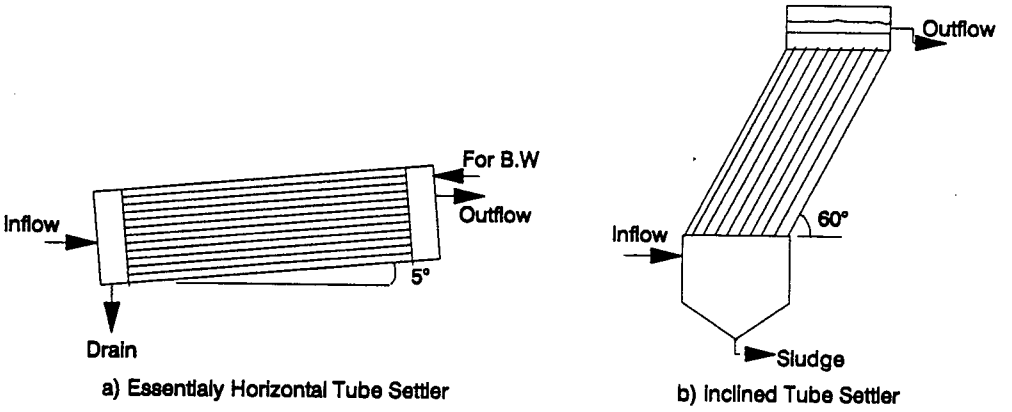

Figure 3.2: Tube Settlers

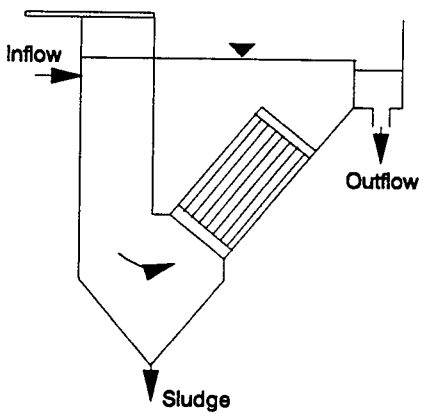

Figure 3.3: Tilted-Plate Separator

the movement of sludge is downwards opposite to the direction of flow. The resistance offered by the flow slows down the movement of sludge, hence requiring high inclination.

In waste water treatment, tube settlers are used in secondary settling and for settling of coagulated wastewaters. They are particularly useful in increasing the capacities of existing final clarifiers. The buildup of microbial slime in the tubes may clog the settlers. In such cases the problem may be minimized by using air to scour the deposits.

The other type of high-rate settler is the Tilted-Plate Separator. It consists of inclined parallel plates spaced closely. For separation of solids from liquid, the upflow type

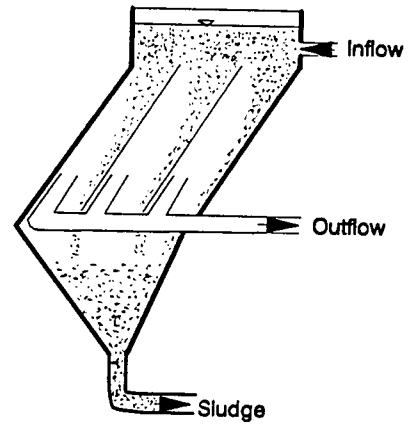

Figure 3.4: Lamella Separator

separator is used. The setup is indicated in Fig. 3.3. It has been reported, Yao('73), that the Tilted-Plate Separator needs less than one-sixth of the floor area compared with plateless separators and to remove particles larger than 10 microns.

Another type of shallow settling device available is Lamella Separator. The name was first introduced in the market as a trademark. Lamella separator consists of inclined parallel plates with typically $25mm$ to $50mm$ spacing. The separator is essentially similar to inclined tube settlers, except that inclined plates are used instead of tubes and the flow of sludge is cocurrent with the flow of water instead of being countercurrent. As shown in Fig. 3.4, the main flow and movement of sludge is in downwards direction. Therefore, instead of the sludge moving opposite to the flow and experience drag resistance it is actually helped by the flow to move downwards. As a result inclination angle of 30° may be used unlike for the inclined tube settlers, hence efficient use of surface are available. This is supposed to be the chief advantage of Lamella Separators. It is recommended by the manufacturers to use it only with coagulated water and wastewater.

3.1.3 Discussion of Theoretical Study

The basic theoretical analysis of high-rate sedimentation has been given by Yao. The analysis is given for sedimentation process in pipes, square conduits, shallow open tray, uniform flow and flow between parallel plates. The theoretical derivations are discused with experimental results obtained by Yao('73).

Yao made the assumptions that the flow is laminar and two-dimensional, particles are discrete and inertia effect is negligible (no particle acceleration). The inlet and outlet conditions are also idealized. The various parameters involved in the theoretical analysis are, settler length, settler inclination, and lateral dimension of settler.

Combining the effect of fluid drag resistance and gravitational settling on a particle, the equation of motion is formulated to obtain family of trajectories and to analyze the effect of different parameters. Assuming a constant concentration along the vertical at the inlet section, removal ratio of sediment is also determined. But, paradoxically, the expression of sediment removal ratio for open tray flow and flow between parallel plates at zero inclination indicate the same result as ideal rectangular sedimentation basin; even though the velocity distribution along the vertical are different.

3.2 Sedimentation Basins

The design of sedimentation basins is based on the type of sediment suspended , the smallest sediment size to be removed, and the degree of removal required. The maximum velocity is limited to a critical value to prevent the pick-up of settled sediments.

There are many different types of sedimentation basins in use. Rectangular and circular sedimentation basins are more popular. The use of vortex-type sedimentation basins has been reported in wastewater and hydro-power plants.

3.2.1 Rectangular Sedimentation Basins

Rectangular sedimentation basins are essentially rectangular box shaped, with the longer dimension in the direction of flow. They may be constructed with or without top cover. A sedimentation basin may be divided into three major regions; inlet, basin area and outlet. Each part needs to be designed for maximum efficiency of sediment removal. From the constructional point of view, rectangular sedimentation basins may be divided as classical type and automatic type. In the classical type, the basin has different compartments, and the operation and flushing of each compartment is done in turn. In the automatic type, which is often known as Deflour sedimentation basin, the continuous flushing of sediment trapped in a sand trap grate, located at the bottom, enables permanent operation of the basin.

Inlet and Entrance Conditions

The inlet conditions of flow and sediment has an influence on the performance of sedimentation basins. The purpose of the inlet is to provide a proper condition for maximum sediment deposition in the basin. Sarikaya's work suggest that a uniform flow velocity with low turbulence level increases the basin efficiency. For this purpose various devices such as weirs, deflecting plates, stilling devices and screens may be used. In waste water treatment, possible floc break-up is to be avoided at the inlet.

The natural way of achieving uniform velocity is by having high inlet energy loss. This idea was used by Camp(Larsen('77)) to estimate the associated uniformity of flow as a function of inlet energy loss. Installing screen at the inlet to basin tend to reduce the sediment transport capacity of a stream. This enhances the deposition of sediments. Experimental work done by Bayazit('71) indicates that fine screens are effective in reducing turbulence, which means high deposition at upstream region. Coarse screens,

conversely, tend to scour the bed. The experimental work also indicates that maximum stable deposition with fine screens to occur by using vertical screen and another downstream facing inclined screen together. Skimmer walls with little submergence are found effective to reduce the turbulence level. Two parallel rows of alternately placed vertical bars are able to reduce the macro scale turbulence and small scale turbulence found in small eddies. The use of a "honey comb" like obstruction in open-channel flow was studied by Aydin(Çeçen('77)) and his experiments show a reduction of turbulence level about $30 - 40\%$. Discussion on the design of sedimentation basins with emphasis on waste water treatment is given by Larsen et al.('77).

The sediment distribution along the vertical at the inlet has an effect on the amount of sediment deposited in basin. It was shown by Hippola('73) that assuming a triangular concentration distribution at inlet to basin reduces the length of sedimentation by $30 - 40\%$. The numerical work of Bechteler et al. shows that the removal ratio of sediment is higher for triangular sediment distribution than for uniform sediment distribution at the inlet.

The Basin Area

The deposition of sediments occur in the rectangular basin area. Basins with shallow depths have low cost of construction and are easy to construct. But, the deposition occurs mostly near the inlet section, within short distance, and may fill the basin in a short period. Therefore, the depth is to be chosen between certain interval. A high-velocity central current is also observed between dead spaces and vortices, instead of uniform velocity distribution throughout the basin length. This phenomenon which is called recirculation or hydraulic short circuit is to avoided for efficient removal of sediment. The inlet and outlet conditions are important factors for the happening.

The analysis and design of rectangular sedimentation basins has been done by many

investigators. The simple formulation is given by ideal rectangular sedimentation basin which assumes idealized conditions. Camp('46) based on Dobbins('44) analytical work has developed a design procedure which includes the effect of turbulence on sedimentation process. But it is assumed that the flow is uniform and sediment transfer coefficient is constant along a section. The analytical solution was given by solving the sedimentation model (Eq. 2.56), neglecting the horizontal diffusion of sediment. It is discussed by Masonyi('65) that the design procedure is conservative for design particle size below $0.1mm$.

The numerical finite difference solution of the sedimentation model with velocity distribution other than uniform was given by Sarikaya('77). The computation was made for logarithmic and parabolic velocity distribution. Constant sediment concentration was assumed at the inlet. The sediment transfer coefficient distribution for the logarithmic and parabolic velocity distribution was taken as parabolic and uniform respectively. Similar solutions with inlet triangular sediment concentration, which is more realistic has been given by Bechteler et al. The sedimentation process with point source was also analyzed.

The overall effect of turbulence in sedimentation may be taken as reducing the fall velocity of a particle. The effective fall velocity may be assumed as $V_s - V_s'$. Where V_s' is the value by which the quiescent fall velocity is to be reduced to account for turbulence effect. Levin(Masonay('65)) has found that

$$V_s' = \alpha U_0 \qquad [m/sec] \tag{3.4}$$

where α is a coefficient. It is generally agreed by investigators that the coefficient may be computed using $\alpha = \frac{0.132}{\sqrt{H}}$ where H is given in meter. The expression for V_s' may be rewritten as

$$V_s' = \beta \frac{U_0}{\sqrt{gH}} = \beta Fr \tag{3.5}$$

where β is a non-dimensional value equal to 0.413 and Fr is the Froude number of the flow in the basin. Therefore the settling length required is

$$L = \frac{HU_0}{V_s - V_s'} = \frac{HU_0}{V_s - \beta Fr} \tag{3.6}$$

Einstein(Strand'86) developed a method of predicting the deposition of fine particles on a gravel bed. The same procedure have been used to design sedimentation basins. The equations (for same sediment size) used are as follows

$$T = 65.7 \frac{H}{V_s} \tag{3.7}$$

$$L_1 = U_0 T \tag{3.8}$$

$$r = 1 - e^{-0.693 L/L_1} \tag{3.9}$$

$$\tag{3.10}$$

where T is time in seconds for sediment concentration to be half the initial value, L_1 is length of basin over which half the sediment allowed is deposited. The coefficient, 65.7 , was obtained from empirical flume studies. Combining the given three equations

$$r = 1 - e^{-0.01055 \frac{LV_s}{U_0 H}} \tag{3.11}$$

Velikanov(Masonyi('65)) has suggested the use of probability theory for solution of sedimentation process in turbulent flow. He studied the probability of settling of sediment with definite fall velocity within a given length. The probability of deposition or removal ratio (for uniform particle size) is given as

$$r = \frac{1}{H/L}\int_0^{H/L} d(y/L)\frac{1}{\sqrt{\pi}}\int_{-\infty}^{\lambda} e^{-t^2}dt \tag{3.12}$$

where

$$\lambda = \frac{\frac{LV_s}{U_0} - H}{\sigma_y\sqrt{2}} \tag{3.13}$$

and σ_y is standard deviation of vertical deflections from the mean horizontal trajectory of sediment. Based on the above analysis the settling length is given by

$$L = \frac{\lambda^2 U_0^2\left(\sqrt{H} - 0.2\right)^2}{7.51V_s^2} \tag{3.14}$$

where 0.2 is essentially constant, and has the dimensions of $\sqrt{L}$.

Shamber et al. ('84) made a numerical analysis of flow in sedimentation basins by using Galerkin finite element method to solve the general transport equations of motion. The structure of turbulence was represented using eddy viscosity concept, the k-ϵ model. Realistic inlet and outlet conditions were incorporated in the solution. The velocity field obtained may then be used further for modelling sedimentation process. Complete simulation of flow and sedimentation process in primary clarifiers was made by Abdel-Gawad et al.('85). The model developed was tested against the measurements obtained in the rectangular clarifiers used in the city of Sarnia, Canada. The method employs the Strip Integral Method (SIM) to solve the general transport equations. They discuss that the SIM is advantageous over the finite element and finite difference model, because of computer time and storage saving. The optimum design procedure considering possible resuspension of deposits is given by Takamatsu et al.('74).

As an outlet device weir or sluice may be used to keep the water level in the sedimentation basin constant and to check water from outlet flushing canal returning back. The use of high weir is to be avoided to eliminate undesirable vortex formation, which directly reduces the basin efficiency.

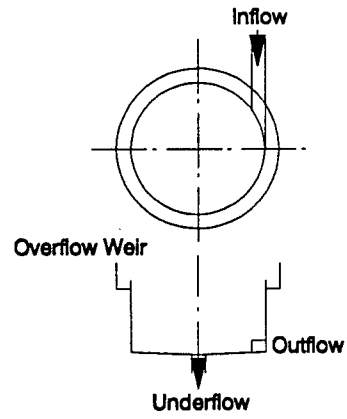

Figure 3.5: Salakhov-type Vortex Settling Basin.

3.2.2 Vortex-type Sedimentation Basins

The classical sedimentation basins works on the principle of providing low flow velocity and turbulence for particles to settle to basin bottom. The settling area required in many cases is so large that its construction may be uneconomical or not feasible. Moreover, the cost of operation and maintenance is high. Sedimentation in water treatment with flocculation requires expensive coagulants, mixing devices and other equipment. As an alternate to conventional sedimentation basins, to eliminate the drawbacks, a circular settling basin with vortex motion has been developed. A vortex-type settling basin is a mechanical separator which uses the effect of flow vortices created by an orifice at the center to collect and flush sediments with little amount of water. Preliminary investigations of the settlers are given by Çeçen('77). Mashauri('86) has reviewed existing different variations of vortex-type basins with his own study included. Different vortex-type settlers are discussed below.

The Salakhov-type vortex settling basin is a circulation chamber with tangential inlet and peripheral weir outlet. The illustration is given in Fig. 3.5. The chamber was used to remove coarse sediments from steep sloped river with high sediment load.

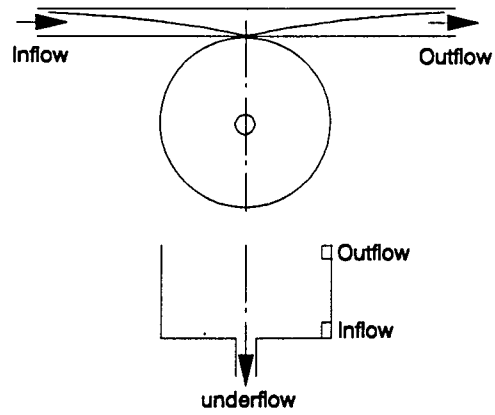

Figure 3.6: Çeçen-type Vortex Settling Basin.

Sediments travel along a spiral trajectory to the chamber bottom due to secondary flow created by the circular motion of the flow. The tangential velocity increases with decreasing radius, which is a characteristic of free vortex flow. For design purposes recommendations are given by Salakhov (Mashauri('86)).

Çeçen('77) has studied vortex type settling basins with tangential inlet and different types of outlet and basins bottoms. Illustration of the basin is given in Fig. 3.6. It is explained that solid particles move to the central underflow due to nonuniform centrifugal forces along a vertical created by frictional fluid deceleration at the bottom. A particle entering the basin takes a helicoidal path towards the underflow orifice, hence the settling length is larger than the dimensions of the basin. This increases the removal ratio for a given sedimentation area compared with the rectangular basin.

Flow conditions near the inlet and outlet are forced vortex, since the tangential velocity increases with radius. Near the orifice underflow the tangential velocity increases with decreasing radius, because of free vortex. Basins with dominant forced vortex flow have higher sediment removal ratio. It is desirable to have an air core in the orifice underflow for reduced flushing discharge. Basins with sloping floor tend to increase the

orifice discharge due to increased water depth at the center. Basins with tangential outlet produces a stronger vortex motion to separate sediments from the flow.

Other variations which use vortex flow as a basis for sediment separation are Sullivan-type and Hydrocyclones (Mashauri('86)). Hydrocyclones are capable of separating solids of size 2 to 200 μm from liquids. The running cost is relatively high due to use of pumps to create the necessary operating head. The Sullivan-type settling basin is commonly used in water and wastewater treatments. Wilson('86) has coupled the free vortex energy dissipation with sediment control, to remove abrasive sediments entering wastewater treatment plant and sewer overflows. He reports that the area required to remove 30 micron sand is less than 5% compared with conventional settling basin.

Generally, vortex-type settling basins have economical advantage over the conventional sedimentation basins. It may be used as pre-settling basin in hydro-power plants for separating coarse sediments to reduce the load entering the main sedimentation basin. The dimensions and the flushing discharge are smaller. The operation is continuous with minimum maintenance.

Chapter 4

SETTING TANK FOR FISHERIES

4.1 Introduction

This chapter discusses the experiments conducted to obtain a suitable geometrical configuration for uniform flow distribution in a high rate sedimentation tank used with fish rearing units.

For effective performance of a high rate sedimentation tank the flow distribution in the structure has to be uniform, because a uniform flow distribution minimizes the flow velocity, thereby maximizing the opportunity for sediment to settle out of the flow. Experiments were conducted to obtain the most suitable geometric system to achieve uniform distribution. The main problem to overcome was the heavy circulation present in the sedimentation tank, which gave quite high velocities around the outer part of the settling basin, these velocities being considerably increased by the repeated recirculation of the fluid.

In a fish rearing tanks it is necessary to circulate fresh water for effective growth of fish. The wastewater from the tanks contains fine organic particles which need to be removed before the water discharges to the stream system. One of the wastewater treatment procedure to remove particles is sedimentation process. The problem in small sized sedimentation tanks is recirculation. Recirculation occurs when some of the fluid passes through the settling zone of a tank in less time than the detention period. It is caused due to non-uniform velocity distribution and difference in length of streampaths.

Due to the high velocity of flow in some part of the tank sediment escapes with the outflow. To avoid recirculation and for the maximum efficiency of sedimentation tank the flow distribution has to be uniform.

The main particles present in a fish rearing effluent are fish manure and uneaten fish feeds. The particles have the tendency to decompose with passage of time. Moreover the physical property changes with time. The particles also have the tendency to stick to rough surfaces and edges, and this makes it difficult to have small openings in the sedimentation unit since such openings can be easily clogged.

The high rate sedimentation tank contains a number of horizontal parallel plates. These horizontal plates are used to increase the surface area of the boundaries, which dampens turbulence and encourages sedimentation in the developing boundary layers on each plate. The opportunity for sedimentation is therefore greatly increased. The uniform flow distribution is also necessary to have equal amount of flow within each settling plate. The inlet and outlet conditions of the tank are arranged to fit in with the operational requirements the whole system; settling and rearing tank.

Previous work has been done on high rate sedimentation tanks. One example is a Lammela separator(Yao('73)). But the problem with the previously designed systems is inability to clean or wash deposited particles on the settling plates. Moreover in some of the systems pumping is required which in this case would disturb the settling of particles and would induce turbulence affecting the overall efficiency of the system. Some of the previous high sedimentation units rely on the self cleansing of the sediments by providing sloping sedimentation surface, but this only works for non-cohesive sediments and is not suitable for the sediment encountered in fish rearing which is highly cohesive and does not have the ability to clean by itself.

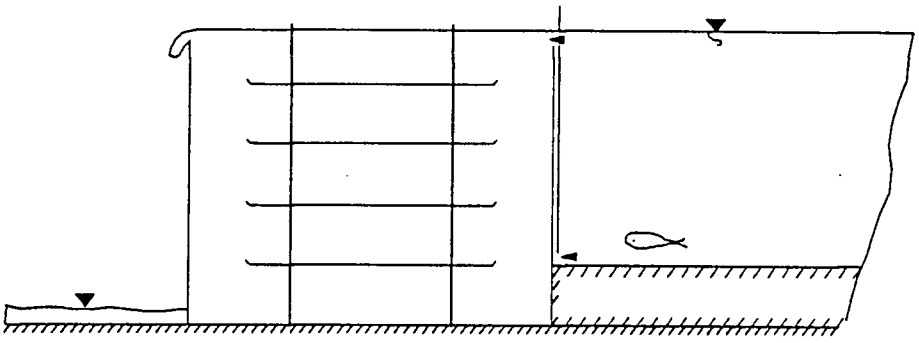

Figure 4.1: Side view of sedimentation unit

4.2 Components of the Sedimentation Unit

The sedimentation unit has four different components; inlet, distributing system, settling plates and control weir outlet. Each component is described as follows.

4.2.1 Inlet

The effluent from the rearing tank is directed through a slot at the bottom of the approach channel as shown in Fig. 4.1. Flow enters this slot and is then forced upwards with high velocity between two plates. These plates are required to separate the rearing tank and the sedimentation tank completely. This separation helps to reduce any disturbance occurring in the settling tank during operation. Moreover the use of mesh or grid for separating the units is discarded since it can get clogged easily. The slot opening at the bottom was proportioned so that the velocities would be high enough to pickup bigger sediments from the rearing tank bed.

The disadvantage with this kind of inlet is that the flow is highly concentrated; and emerges from the top of the plates at B, Fig. 4.2, with high velocity, and this crates problem for flow distribution. This high velocity at entry to the settling basin causes flow in the settling tank to recirculate. Moreover turbulence is induced into the system

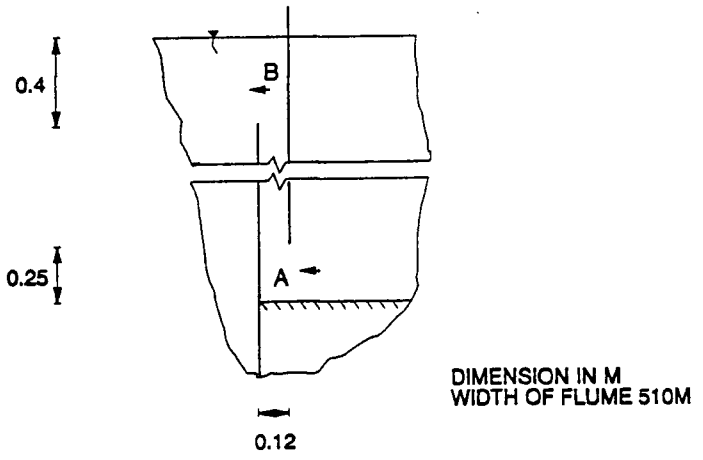

Figure 4.2: Inlet side view

and the flow is not distributed to the various plates.

The Reynolds number for flow in the slot is given by

$$Re = UD/\nu \qquad (D = 4R) \tag{4.1}$$

where U is velocity, R is hydraulic radius, and ν is kinematic viscosity. For a given maximum flow of $.85m^3/s$, opening area of .012×.51m, and assuming wide rectangular channel,

$$Re = \frac{.85 \times 10^{-3} \times .012 \times 4}{10^{-6} \times .012 \times .51 \times 2} = 3333$$

which indicates that the flow is turbulent within the slot.

4.2.2 Distributing System

Different systems were tested during the experimentation to achieve uniform flow distribution within the settling tank. Two of the systems tested will be described here. In the first one shown in Fig. 4.4 deflectors were placed at different levels, with the purpose of deflecting the flow directly in line with and towards the plates. The second one Fig. 4.3 uses the principle of dissipating the incoming energy and directing the flow at an angle towards the plates. Each type is discussed below.

Grated System

The circulation in the tank is by the incoming high velocity flow from the slot opening. Since the outlet from the tank is near the water surface, there is a tendency for the flow to concentrate within the top portion of the settling tank. In order to avoid the high momentum flow coming out from the slot and hence the heavy circulation, an energy dissipation mechanism has to be arranged. Moreover the flow has to be deflected at an angle to the plates. In order to achieve the above mentioned processes three layers of a grating formed from metal strips were used. The openings of the grate were staggered to get the maximum energy dissipation.

Different trials were made using different spacings between the layers and different percentage of opening for each layer. For the spacing a limit is reached that it is no longer feasible to clean the metal strips.

Plate Deflectors

As discussed before without any arrangement at the slot outlet, the flow concentrates within the top portion of the tank. To avoid this a baffle, was constructed to divert the flow downwards, to the deflecting plates, as shown in Fig. 4.4. These deflecting

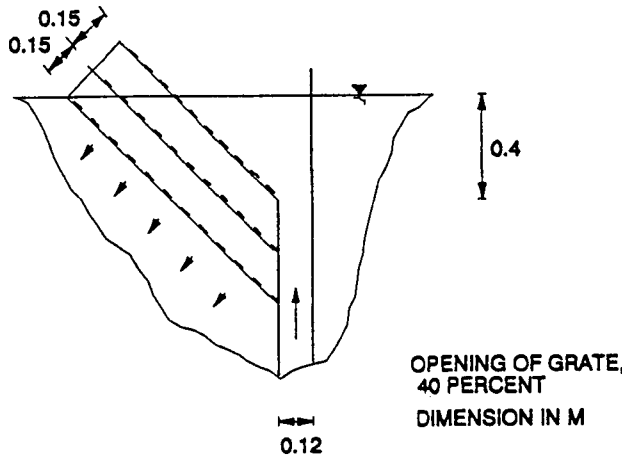

Figure 4.3: Grated system side view

plates are used to divert the flow directed downwards by the baffle at right angle towards the settling plates. The deflecting plates are arranged at different levels to deflect the flow horizontally at these various levels of the tank section. If designed correctly, this deflection of flow at various evenly distributed depths achieves a uniform flow distribution through the settling plates.

The dimension of the deflecting plates is very important in determining their deflecting capacity. In the experimental work it was seen that the width to length ratio (aspect ratio) is the determining factor in the effectiveness of the plates. The flow deflected from the plates tends to have a downward movement before it reaches the plates. If the length of the deflecting plates in the flow direction is short, it is likely that the distribution of the flow is not uniform. Therefore the optimum length of the deflecting plates was to be determined. This length is also important for the top settling plate, because a proportional amount of flow has to be deflected towards the top settling plate before the flow gets deflected downwards.

The deflecting plates are arranged in a staggered manner between each row. This

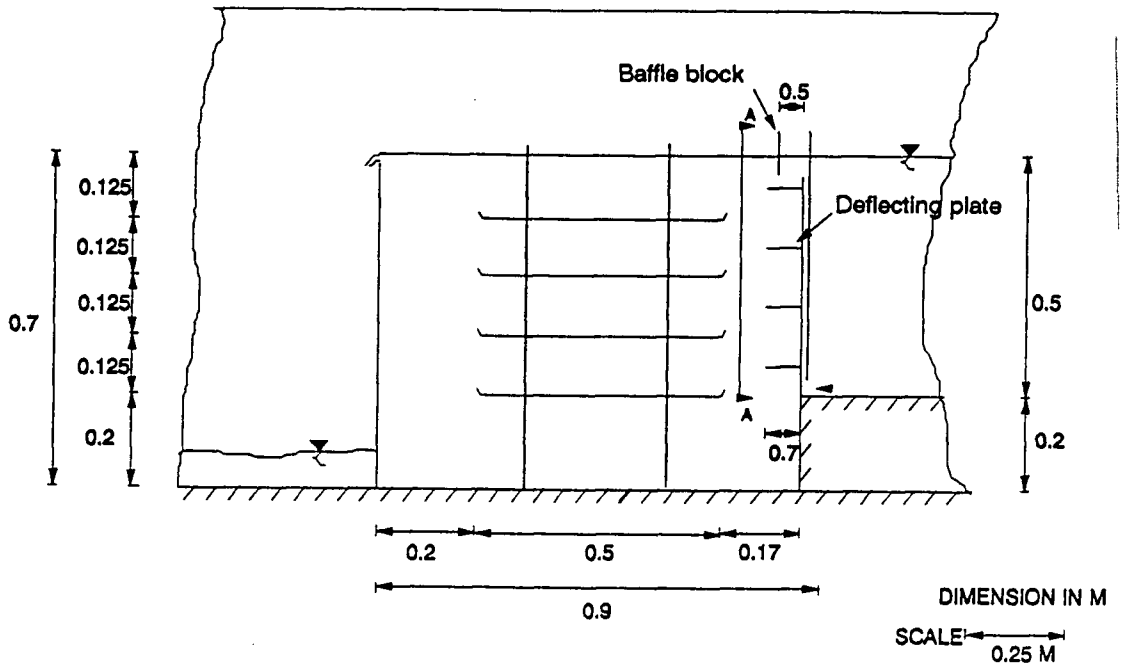

Figure 4.4: Sedimentation tank side view

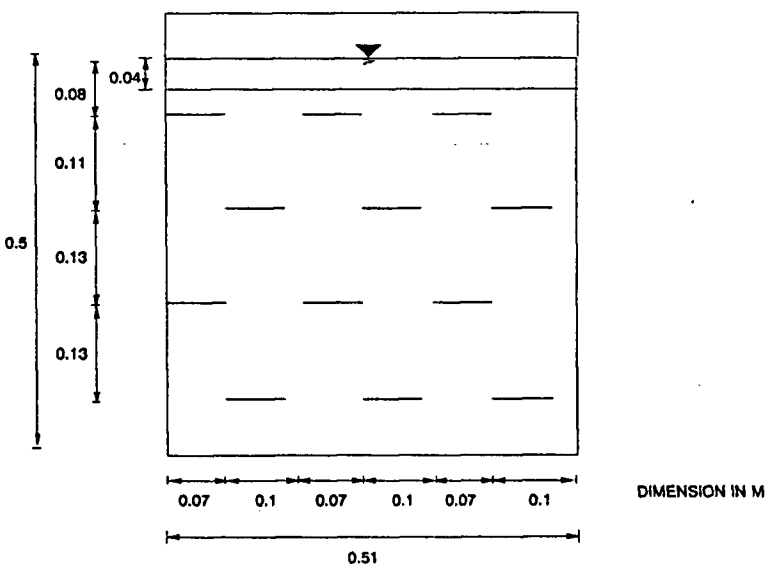

Figure 4.5: Deflecting plate arrangement

enables each row of deflecting plates to take a proportional amount of flow with respect to the widths of the plates. The staggered arrangement as indicated in Fig. 4.5 gave a better flow distribution. The plates apart from acting as deflecting devices; they created resistance to the flow moving downwards deflected from the baffles. This enabled the high velocity deflected flow to slow down and distribute itself horizontally.

The dimensions of the deflecting plates and the relative position and arrangement of the deflecting baffle were determined after a lot of trial and error experimentation. The top settling plate and at times the bottom settling plate were critical in determining the dimensions.

4.2.3 The Settling Plate System

The design of the settling plates was based on the loading rate or on the removal of sediment of specific settling velocity. For this case the loading rate was taken as $9.26 \times 10^{-4} m^3/(m^2 - sec)(80 m^3/(m^2 - day))$. The width of the plates is fixed by the width of the rearing units. Moreover the length of the plates along the flow direction is dependent on the space available for sedimentation tank. The main design objective is then determining the number of plates required. The following are given values for design,

Design maximum flow $= .85 \times 10^{-6} m^3/s$

Design minimum flow $= .425 \times 10^{-6} m^3/s$

Width of tank $= 0.51$ m

Length of plates $= 0.5$ m

$$Surface\ area\ required\ = \frac{flow\ rate}{loading\ rate} \tag{4.2}$$

substituting the corresponding values,

$$\text{Surface area required} = \frac{51 \times 10^3 \times 1440 \times 60}{60 \times 80}$$

$$= 0.918 \text{ m}^2$$

$$\text{Number of settling plates required} = \frac{.918}{.51 \times .5} = 3.6$$

Therefore 4 settling plates to be used.

Spacing between each plate = 0.50/4 =0.125 m

When the flow rate is low as indicated by the minimum flow, the number of settling plates required is less. Since at low flow all the provided plates are not necessary, the uniform distribution of flow is not critical. Therefore high consideration was given for high flow rate.

The settling plates were arranged horizontally and parallel to get the maximum possible settling surface area within the provided space. The cleaning of the plates is to be performed by rotating the whole plate system at right angle. Therefore an extra space is required below the bottom plate to enable the whole system of plates to rotate. In fact this extra space provides extra sedimentation area. Since the distribution of flow in this area is not reliable, it is not considered in the design. This extra space has also advantage of settling bigger particles which would easily fill up the other settling plates. Moreover it compensates the reduction of efficiency of the plates due to any change of flow phenomenon from the idealized case.

It is necessary to check whether the flow in the plates is laminar so that tranquil settling is facilitated.

Assuming a laminar boundary layer development we have,

$$\delta = \frac{4.91 \times x}{\sqrt{Re_x}} \tag{4.3}$$

substituting the corresponding values,

$$\frac{.125}{2} = \frac{4.91 \times x}{\sqrt{\frac{x \times 8.5 \times 10^{-4}}{10^{-6}}}}$$

solving, x =.14m , hence the flow develops within the plate.

If a turbulent boundary layer is assumed,

$$\delta = \frac{.37 \times x}{Re_x} \tag{4.4}$$

substituting the corresponding values and solving, x = .58m which is greater than the plate length (0.5m).

But fully developed region was observed in the experiment. Hence the observation suggests the development of laminar boundary layer.

Considering the Reynolds number of the fully developed region,

$$Re = \frac{UD}{\nu}$$

$$= \frac{51 \times 10^{-3} \times 1 \times 4 \times .125 \times 1}{60 \times 4 \times .125 \times .51 \times 2 \times 1 \times 10^{-6}}$$

$$= 833$$

which indicates that the flow is laminar since less than 2000.

It is obvious that due to the inlet conditions to the settling plates the flow is not totally laminar at the beginning. But it changes to laminar flow as it proceeds further down between the settling plates.

Particles deposited on the plates form a layer. Before washing deposits on the plates, the water in the tank has to be drained. The deposited layer is of loose material which can be disturbed easily. In the process of draining, the deposited material gets disturbed and washed away. From wastewater treatment point of view the deposited material is to be washed and collected separately for further treatment. The drained water from the tank is not to be mixed with the deposited material. To restrict the washing away of the deposited material while draining; the edges of the plates upstream and downstream side are bent upwards. This helps to hold the deposited material from moving away. Nevertheless the flow at the inlet to the plates gets disturbed due to the bend which is not desirable. But from the operational point of view the setup is unavoidable.

The presence of the plates has an effect on the distribution pattern of the flow. Better distribution of flow was observed without the presence of the plates . The relative position of the plates in the tank unit has an effect on the flow pattern. This depends on how far the edge (inlet) of the settling plates is located from the face of the baffle. It doesn't seem that the gap between the downstream weir and outlet of the plates has an effect on the flow distribution pattern.

4.2.4 Control Weir Outlet

The water level in the rearing tank has to be kept at a constant level. The control of the water depth both in the rearing tank and the sedimentation unit is controlled by a sharp crested weir. The head required over the sharp crested weir is very small compared to the depth of flow. Any variation in the flow rate has minimum effect on the head over the weir. With the installation of the crested weir the flow is concentrated at the

top section of the tank. Without flow distributors it contributes to the high circulating tendency observed in the system. No special arrangement is made near the crested weir for uniform flow distribution. The efficiency of the whole system is dependent on the structure constructed near the baffle or the inlet to the settling tank.

Chapter 5

DEVELOPMENT OF THEORY

Many investigators have attributed the process of suspension to the turbulent fluctuating of fluid flow, Garde et al.('85). Bagnold('66) discusses that, near a solid boundary, the turbulent shear flow causes an anisotropic turbulence which is responsible for supporting sediments in suspension. In an anisotropic turbulence the upward and downward fluctuating turbulent velocity intensities are different in magnitudes so that there is a net stress away from the boundary. Bagnold('66) illustrates this idea with flow visualization photographs of flow near a solid boundary surface taken by Prandtl('52).

Bagnold considers a unit volume of fluid above a horizontal surface and evaluates the net upward momentum flux with respect to upward velocity fluctuation. Within the elemental volume the conservation of mass is satisfied. After maximizing the momentum flux, he relates it to the rms of the vertical velocity fluctuation, which gives,

$$f = 0.414\rho\overline{v'^2} \tag{5.1}$$

where f is momentum flux and v is vertical velocity fluctuation. The maximum value of $\sqrt{\overline{v'^2}}$ near the wall must be able to support the whole suspension up to the free surface, and from Laufer's ('51) experimental results the ratio $\sqrt{\overline{v'^2}}_{max}/U_*$ is approximately equal to unity. Therefore expressing the net momentum fluctuation with respect to the boundary shear stress, τ_w, which by definition equals ρU_*^2,

$$f = 0.414\tau_w \tag{5.2}$$

After further analysis he gives the sediment carrying capacity of a flow, in terms of efficiency with respect to the total stream power. It is to be noted that Laufer's experimental result is given for flow over a smooth boundary.

Bagnold compares his result with the work of Irmay ('80), which uses a totally different approach, for the confirmation of his result. Irmay's analysis uses the simplified form of the Navier-Stokes equation for turbulent steady two-dimensional fully developed flow. For fully developed two-dimensional flow the variation of flow variables is in the vertical direction only. Irmay derives the acceleration term of a fluid particle in the vertical direction in terms of the pressure variation and hence to the vertical velocity fluctuation after simplifying the Navier-Stokes equation as follows

$$a_y = -\frac{1}{\rho}\frac{\partial p}{\partial y} = \frac{\partial \overline{v'^2}}{\partial y} \tag{5.3}$$

Bagnold integrates the acceleration term to obtain the net upward momentum flux in the fluid flow. Therefore

$$f = \rho \int_0^y \frac{d\overline{v'^2}}{dy} dy = \rho \overline{v'^2}_{y=H} \qquad (since\ \rho \overline{v'^2}_{y=0} = 0) \tag{5.4}$$

But Irmay has evaluated the ratio $\frac{\overline{v'^2}}{U_\tau}$ verses y/H, using Laufer's fully developed smooth boundary experimental result. From the analysis it is shown that the value $\rho \overline{v'^2}_{y=H}$ is given by $0.375\tau_w$ (approx.). Substituting the result into Eq. 5.4,

$$f = 0.375\tau w \tag{5.5}$$

from which Bagnold concludes that the above result is in good argument with his derivation given by Eq. 5.2.

The main objective of this study is to extend the whole idea discussed above to sedimentation in closed conduits. It can be seen clearly from Eq. 5.4 that the supporting

stress from the net momentum flux depends on the value of $\rho\overline{v'^2}$ in the limit considered. At the lower solid boundary it is obvious that the value $\rho\overline{v'^2} = 0$. If an upper boundary is introduced, the same value $\rho\overline{v'^2}$ tends to be equal to zero, hence from Eq. 5.4 there would not be net sediment supporting momentum flux.

Viewing the whole situation from another angle, if the lower smooth boundary is responsible for the turbulence production and hence an upward momentum flux then a solid upper boundary would be expected to exert a downward momentum flux to push the sediments downwards. Which is to suggest that the net sediment transport with solid upper boundary would be zero. Hence a sedimentation basin with top solid boundary would be expected to have higher efficiency than the equivalent basin with free surface. For rough solid boundary the rms of the vertical velocity fluctuation is found to be higher than for smooth solid boundary, Hinze('59), Blinco et al.('72), McQuivey et al.('69), hence higher momentum flux, hence higher momentum flux. Actually the non dimensional turbulence intensity is more or less the same for both rough and smooth boundaries. But for the same flow case the shear stress for the rough boundary is higher than that for smooth; therefore the turbulence intensity is higher. From the above discussion, a rough solid upper boundary is expected to generate more turbulence and hence higher downward momentum flux than the smooth solid boundary at the bottom. The net downward push on the sediments would be expected to facilitate the sedimentation process.

Chapter 6

NUMERICAL MODELLING OF FLOW AND SEDIMENTATION

The analytical solution of the general transport equation with different boundary conditions is too involved and impractical, therefore, the numerical solution of the equation is adopted in this study using the Control Volume Method (TEACH[1] code). The solution procedure for the code is given in Appendix B. The turbulent kinetic energy, k, and its dissipation rate, ϵ, are considered as dependent variables. The two variables are solved in the model by successive substitution from the momentum and mass transport computation results. The model is valid only for fully turbulent flow. The wall function (Appendix A) is used to approximate turbulence properties near the wall where viscous effects are more pronounced than turbulent effects.

From the numerical solution of the flow problem using TEACH code, a field of velocity components and viscosity is used for the computation of the sedimentation process. The computer program for the sedimentation model was developed in line with the scalar quantity transportation model, ϕ for k and ϵ in Chapter 2, with the appropriate boundary conditions.

6.1 Physical Model and Boundary Conditions

The physical models used for this study consist of (a) flow between smooth parallel plates, (b) flow between parallel smooth and rough plate, and (c) open channel flow, all with unit thickness. The description with the appropriate boundary conditions is given in

[1]Teaching Elliptic Axisymmetric Characteristics Heuristically

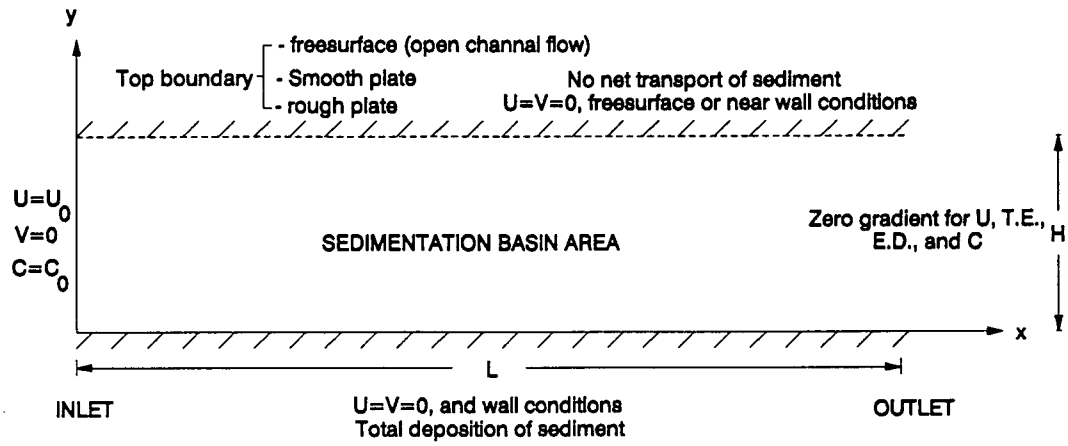

Figure 6.1: Physical Model and Boundary Conditions.

Fig. 6.1. The sedimentation processes in the three flow cases are to be compared.

The boundary conditions are given as follows,

Inlet

- plug flow with essentially small turbulence level, ($U = U_0 = 0.2m/s, V = 0, k/U_0^2 = 10^{-6}, C = C_0 = 1$). All the variables have a constant value across the inlet section.

Boundary

- no slip and no penetration at the plate for flow properties, ($U = V = 0, \frac{\partial k}{\partial y} = \frac{\partial \epsilon}{\partial y} = 0$).

- for sedimentation process, at the bottom boundary, $\epsilon \frac{\partial C}{\partial y} = 0$ since all the sediment reaching the bottom is retained. At the top boundary, since there is no net transport of sediment, $\epsilon \frac{\partial C}{\partial y} + V_s C = 0$.

- the effect of a wall on the flow at an adjacent control volume is implemented using a momentum sink, wall shear stress, in the source term of the finite difference equation; because for the controls volume near the wall, the wall shear stress is treated

as external force in the horizontal momentum flux equation.

Outlet

- all variables have zero gradient, which assumes that fully developed or equilibrium conditions exist. The computation domain is made long enough to justify this assumption.

6.2 Finite Difference Formulation

6.2.1 Control Volume Definition

The conservation equations are solved numerically using the control volume integral approach on a discrete grid. The grid network consists of orthogonally aligned nodes for which the scalar properties (k, ϵ, μ_{eff}, C) are computed. The boundaries for the scalar control volumes are located midway between the nodes. The layout of the computational grid is shown in Fig. 6.2. The point 'P' is a particular node point under consideration and the neighbor nodes to the north, south, east and west are indicated by 'N', 'S', 'E', 'W' respectively. The control volume faces are identified by the lower case letters (n,s,e,w), and the solid lines indicate the boundaries.

The vector quantities, U and V, are defined at the boundaries of the scalar quantity control volumes, between respective grid points. Their control volumes are indicated by dashed lines. The velocity U, at a particular node is defined as being that entering the left side, and the velocity V, as that entering from the bottom side of the control volume. The velocity grids are staggered halfway to the east and south.

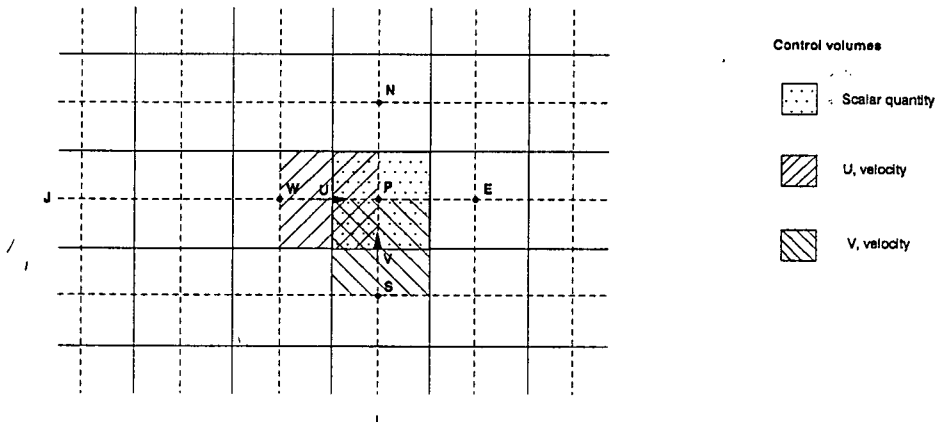

Figure 6.2: Control Volume Description

6.2.2 Derivation of Finite Volume Equations

The derivation of the general finite difference equation is done by integrating the general transport equation given by Eq. 2.45 over its corresponding control volume. Fluid properties within each cell is assumed to be constant and linearly interpolated between nodes to satisfy the continuity of total flux. Integrating Eq. 2.45

$$\int\int \left[\frac{\partial}{\partial x}(\rho U\phi) + \frac{\partial}{\partial y}(\rho V\phi) - \frac{\partial}{\partial x}\left(\Gamma\frac{\partial\phi}{\partial x}\right) - \frac{\partial}{\partial y}\left(\Gamma\frac{\partial\phi}{\partial y}\right)\right] d(VOL) = \int\int S_\phi d(VOL) \tag{6.1}$$

where VOL is volume of the cell considered.

Using the Gauss Divergence Theorem (to replace volume integrals by surface integrals), the above equation may be written as

$$\int_s^n \left[\left(\rho U\phi - \Gamma\frac{\partial\phi}{\partial x}\right)_e - \left(\rho U\phi - \Gamma\frac{\partial\phi}{\partial x}\right)_w\right] dy + \int_w^e \left[\left(\rho V\phi - \Gamma\frac{\partial\phi}{\partial y}\right)_n - \left(\rho V\phi - \Gamma\frac{\partial\phi}{\partial y}\right)_s\right] dx = [S_P\phi_P + S_U]VOL \tag{6.2}$$

where S_P and S_U are linearized source terms.

Considering as an example the east face of control volume, the flux (convective and diffusive terms) is given as

$$F_e = \int_s^n \left(\rho U\phi - \Gamma\frac{\partial\phi}{\partial x}\right)_e dy = \left[\rho U\phi - \Gamma\frac{\partial\phi}{\partial x}\right]_e \tag{6.3}$$

where F_e, is facial flux at the east side of control volume; the subscript indicates the corresponding face. The hybrid differencing scheme is used to express the fluxes in terms of modal ϕ values, depending on the cell Peclet number, Pe, defined as

$$Pe = \frac{(\rho U)_\Delta x}{\Gamma} \tag{6.4}$$

For $|Pe| \leq 2$ central deference is used and for $|Pe| > 2$ an upwind differencing is used. Therefore Eq. 6.3 may be rewritten as

$$F_e = \rho U A_e[f_e\phi_E + (1 - f_e)\phi_P] \tag{6.5}$$

where A_e is area of eastern face of cell. The coefficient f_e is given as follows

$$f_e = \begin{cases} \frac{1}{2}(1 - 2Pe^{-1}) & \text{for } |Pe| \leq 2\ ; \\ 0 & \text{for } Pe \geq 2\ ; \\ -1 & \text{for } Pe < -2 \end{cases}$$

where Pe is evaluated on the east side of the cell. In similar way, the fluxes F_w, F_n and F_s are obtained.

Substitution of the flux and source expressions into the continuity expression (Eq. 6.2) yields

$$a_P\phi_P = a_W\phi_W + a_S\phi_S + a_E\phi_E + a_W\phi_W + S_P\phi_P + S_U \tag{6.6}$$

where a_P, a_N, a_S, a_E and a_W are collected coefficients of $\phi_P, \phi_N, \phi_S, \phi_E$ and ϕ_W. For eastern neighbor, the coefficient a_E is expressed as

$$a_E = (\rho U)_e A_e f_e \tag{6.7}$$

The coefficient for the considered node is given as

$$a_P = \sum_n a_n \tag{6.8}$$

where 'n' represents the face, and ,$\sum_n$, is the summation over neighbours. It is to be noted that for the velocity components the control volumes are displaced from the scalar control volumes. The driving pressures for the velocities are located at each end of a particular cell.

The momentum equations are solved by starting from a guessed pressure field. However, these solutions may not satisfy continuity condition, so that a pressure correction equation is therefore required. To meet the requirements of continuity, the calculated flow velocities are adjusted by calculating the net accumulation of mass and then the correction for local pressure. Integrating continuity equation over the main control volumes

$$|\rho U A|_e - |\rho U A|_w + |\rho V A|_n - |\rho V A|_s = 0 \tag{6.9}$$

where 'A' denotes area. Expressing the velocities in terms of pressure

$$U_E = U_E^* + \frac{\partial U_E}{\partial (P_P - P_E)} (P'_P - P'_E) \tag{6.10}$$

where U_E^* is velocity corresponding to guessed pressure field, P^*, and P' is the pressure correction. Substituting for velocity in continuity equation, the finite difference equation for pressure correction is

$$(a_P - S_P)P'_P = \sum_n a_n P'_P + (\rho U^* A)_e - (\rho U^* A)_w + (\rho V^* A)_n + (\rho V^* A)_s + S_U \quad (6.11)$$

The U-momentum finite difference equation incorporating pressure correction is given as

$$(a_P - S_P)U_P = \sum_n a_n U_n + S_U + A_e(P_W - P_P) \quad (6.12)$$

The algebraic equation given by Eq. 6.6, which links the nodal ϕ value with the surrounding ϕ's is established for all nodal points in the computation domain. Solution is obtained by using 'Line by Line' method, which is described below

- equations are formulated as $(a_P - S_P)\phi_P = a_W\phi_W + a_S\phi_S + S'_U$ where $S'_U = a_W\phi_W + a_E\phi_E + S_U$, which is temporarily taken as known.
- solution along N-S line is obtained using Tri-Diagonal Matrix Algorithm (TDMA).
- solution along neighoring line is obtained using recently calculated ϕ and S_U values.
- the domain is swept repeatedly until the desired solution is obtained.

6.3 Solution Algorithm

To obtain complete solution of the flow and sedimentation process problem, the algebraic equations are formulated for all dependent variables. The solution procedure adopted in TEACH code is the SIMPLE[2] algorithm. The sequence of operation is as follows

- pressure field is guessed.
- momentum equations are solved using guessed pressure values.

[2]Semi-Implicit Method for Pressure Linked Equations

- pressure is calculated based on pressure correction equation.

- velocities are calculated based on velocity correction formulae.

- conservation equations for other properties are solved (turbulence quantities). The sediment concentration solution is obtained after flow field solution.

- the corrected pressure is treated as guessed pressure and the whole procedure is repeated until desired convergence is obtained.

6.4 Convergence Criteria

The numerical solution of the established finite difference equations is obtained by iteration. All equations satisfy the necessary conditions that

$$|a_P - S_P| \leq |a_N| + |a_S| + |a_E| + |a_W| \text{ provided } S_P \leq 0 \tag{6.13}$$

The momentum equations are non-linear by nature. This requires the under-relaxation of the velocities. The under-relaxation factor is usually 0.5.

The degree of convergence is measured by checking how well the solution satisfies the finite difference equations so that the residual error for each variable is given as

$$R_\phi = (a_P - S_P)\phi_P - \sum_n a_n\phi_n - S_U \tag{6.14}$$

The absolute residual for the whole domain is obtained by summing, $\sum |R_\phi|$. In addition, among the variable residuals, the highest value is checked not to exceed the maximum error allowable.

Chapter 7

EXPERIMENTS

7.1 Objective of Experiments

The main objective of the experiments was to study the effect of a introducing top solid boundary on the performance of sedimentation basins. It was to investigate experimentally the suggestion presented in the previous section that a top solid boundary is able to exert a downward push on the solid particles and hence facilitate the settling of particles. It was also required to check how far a rough top boundary is able to affect the efficiency of sediment removal of a sedimentation basin. The effect of positioning a solid boundary at half the depth from the bed of the basin was also investigated. The different set-ups employed are discussed as follows.

Five different arrangements were necessary to conduct the study. The first experimental set-up was to study the deposition of sediment with free surface for the upper boundary and this result will be used to compare with other experimental results. The second experiment was conducted to study the effect of a smooth plate placed at half the free surface flow depth. The third and fourth experiments are similar to the second experiment except that two different types of roughness were used to study the effect of a rough boundary on the deposition pattern of sediment in a sedimentation basin. The fifth experiment is similar to the first experiment except that the depth of flow was halved and was conducted to compare with the second experiment to check whether the solid boundary helped to increase the efficiency of the basin.

7.2 Apparatus

The experiments were conducted in a flume 0.51m wide, 1.0m deep, and 13.2m long, without recirculating the flow. The flume has an adjustable slope. The bed level was kept horizontal throughout the experiment. The flume bed was covered with strips of aluminium plates (1mm thick) 0.1m wide in the flow direction. Details are given in Fig. 7.1.

For the closed conduit experiment, an aluminium plate (3.4mm thick) was used as a top cover. For the smooth top plate experiment, the plane aluminium plate was used. For the rough top plate experiment, two roughness types were used. The first roughness material selected was sand of 1.3mm mean size. The top aluminium cover was painted and the roughness material spread uniformly. The second roughness material adopted was a 5mm gravel. Instead of using paint directly on the aluminium plate, latex glue was applied on a plywood and the gravel material spread uniformly. Then the plywood was fixed to the top plate. The top boundary was made water-tight by fitting rubber along the plate edge where it comes in contact with the flume wall. It was observed that no leakage happened throughout the experiment.

The test section was set up at 8.1m from the inlet of the flume. This was made long enough for the flow to be well developed. At the inlet wire mesh screens were where arranged to dampen any disturbances and stabilize the flow.

The sediment was fed as a wet slurry into the flow using eight 4.8mm diameter plastic pipes placed horizontaly, 50mm above the channel bed. The suitable pipe size for even distribution of flow was selected by trial. The sediment water mixture was fed using a peristaltic pump with the outlet plastic pipe 8.0 mm diameter distributing equal amount of flow to the eight feed pipes. The detailed arrangement is shown in Fig. 7.2b. The peristaltic pump used was Cole-Parmer made of type 7018 with total discharge capacity of

50ml/sec. Sand of .11mm size was used as sediment particle throughout the experiment.

The sediment water mixture was pumped from a small tank 0.15×0.38 ×0.25mm size. The sediment was kept in suspension within the tank by using a small electric driven stirrer. A constant amount of water supply was provided from an outside source, and an overflow orifice provided a constant water level in the tank. The position from which the sediment water mixture was pumped was kept fixed so that a constant sediment concentration was supplied to the flow. The detail of the tank is given in Fig. 7.2a.

7.3 Procedure

A sill downstream of the flume provided a control section to keep the required depth of flow of 0.1m. The velocity of flow was chosen to be 0.1m/s to match with the practical range of values used in the design of sedimentation basins and to keep a reasonable settling length within the channel for the sediment size selected. Water to the flume was supplied at a constant rate of $0.005m^3/sec$ from an external source. Water was allowed to run in the flume for about five minutes for the flow to develop fully.

Before flow is allowed to the flume, 24 aluminium sheet metal strips (0.1m×0.51m) and one 0.2m×0.51m (near feeding area) were spread on the flume bed of the test section. Sediment feed pipes were fixed securely at 0.05m (half the depth) above the flume bed and then, for the top solid boundary experiments, the aluminium plate is placed in position. Flow distribution in each feeding pipe is checked for even supply of sediment across the channel width. Throughout the experiment, satisfactory feeding of sediments was observed. Sediment and water mixture in the feeding tank is stirred well before the experiment is started till sediment concentration equilibrium is reached.

For each different cases of set-up, the experiment is started by pumping the sediment-water mixture once the main flow is fully developed. Each experiment was run for exactly

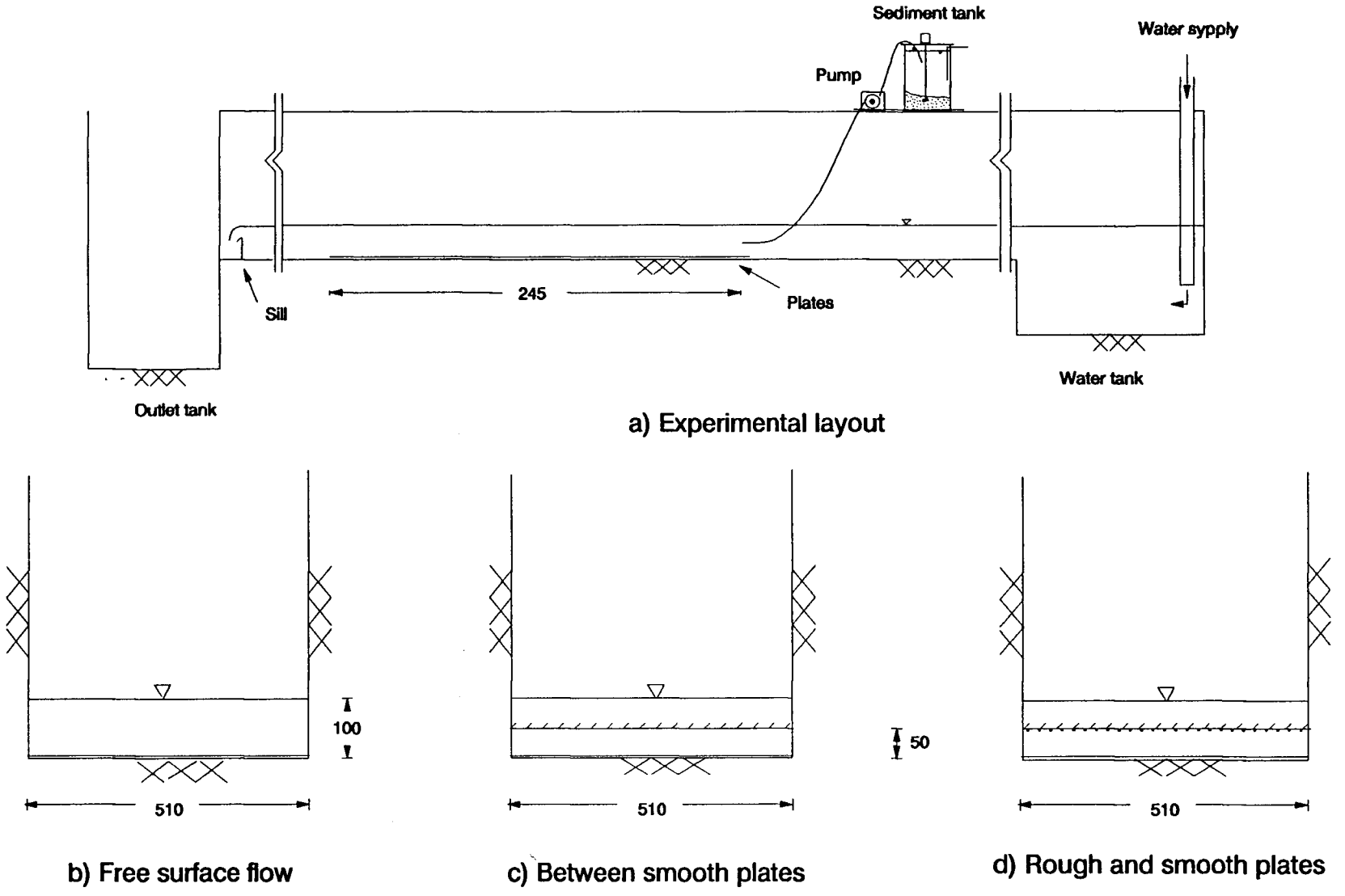

Figure 7.1: Experimental setup

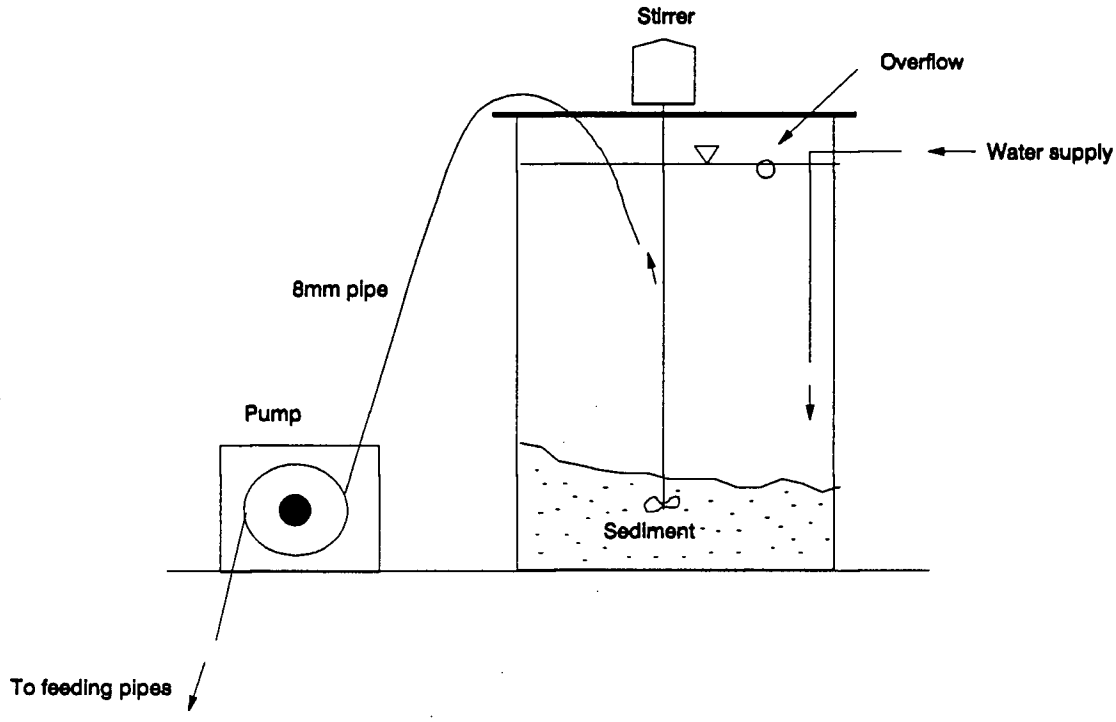

a) Sediment feed tank

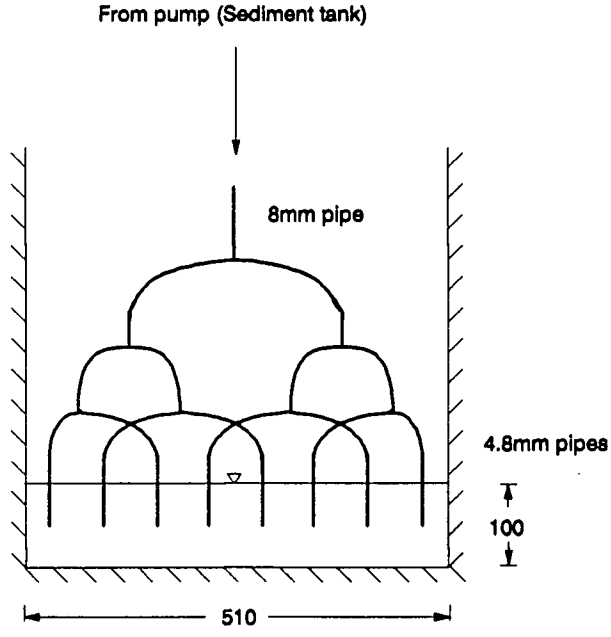

b) Sediment feeding pipes

Figure 7.2: Sediment feeding system

10 minutes. Thereafter the pumping was stopped and the water supply to the flume was slowly reduced to avoid disturbance of settled material. After draining the whole flume, the plates with the deposited sediments were left to dry by blowing hot air, very gently from an electric fan. The sediment deposited on the plates was weighed using a balance with a least count of 0.01gm.

Chapter 8

EXPERIMENTAL RESULTS

The purpose of the experiments was to determine whether the sediment settling rate could be increased. Any increase would be indicated by changes in the deposition pattern in the basin. However, it was difficult to control the sediment feed precisely, and since the inlet sediment concentration was different, the total amount of sediment deposited was also different. Therefore, to have a common ground to compare results, the settling length and deposition pattern needed to be made non-dimensional. Consequently, results from each experiment are compared using non-dimensional plots.

To make the sediment deposition non-dimensional, the amount of sediment deposited on each plate is divided by the total amount of sediment settled in the channel. The number of plates was made large enough to settle all the sediment fed in at the inlet. The settling length or the position of the plate from the sediment feed point is made non-dimensional by dividing by the depth of flow. Since the depth of flow is not the same for all cases, a reference depth of H=100mm is used to obtain a non-dimensional length. The plotting of the non-dimensional sediment deposition ratio and settling length gives a picture of the sediment deposition distribution, and from these graphs, the deposition pattern for the different experiments can be compared.

For sedimentation basins, the total cumulative amount of sediment removed at each section from the inlet is also of major importance, and this characteristics is defined by the removal ratio, which is the ratio of the amount of sediment deposited at a certain section divided by the total amount of sediment deposited in the basin. At a section

where sediment is completely removed the removal ratio approaches unity.

The longitudinal distribution of sediment along the bed of a settling basin made up of traps is given by Çecen et al.('71). Both the theoretical and the experimental treatments are discussed. Some comparison will be made with these results, but the present experiments are somewhat different because the experimental and numerical work discussed in this study was made using, not traps, but a sedimentation basin with plane bottom and top boundaries.

The parameters for each experimental run is given in Table 8.1. For each type of setup the experiment is done twice to make sure that the first experimental result is almost repeated by the second. To check that the time of pumping and concentration of sediment does not influence the deposition pattern, two different pumping times and sediment concentrations were selected for the same experimental set up. The experiments are indicated in Table 8.1 as run #1 and run #2. As it can be seen from Fig. 8.1, the deposition characteristics do not seem to be influenced. The water temperature range for the experiment was between $4^0C \text{and} 10^0C$. The temperature variation effect on settling velocity as given by Vanoni('75), Fig. 2.9, shows little variation for the range selected. Therefore the difference is ignored.

The deposition and removal ratio of sediment for free surface flow and for flow between parallel smooth plates is given by Fig. 8.1. It is seen from the graph that on average there is not much difference between the type of flows.

Experiment run #3 and run #4 were conducted for a 100mm depth of flow with smooth plate at top. Run #5 and run #6 were conducted with smooth plate positioned at half of the approach flow depth, that is 50mm from the bed. Effectively the depth of flow is 50mm. The sediment deposition pattern for the two cases is given by Fig. 8.2. It shows that a difference exists in deposition pattern. The peak deposition is increased by about 50 percent. The slope of the frequency distribution deposition for the two cases

Table 8.1: Experimental setup parameters

Run #	Conc.(ppm)	Time (min.)	Plate position(m)	Plate type
1	1500	20	-	-
2	5300	10	-	-
3	2900	10	0.1	Smooth
4	4400	10	0.1	Smooth
5	3900	10	0.05	Smooth
6	3700	10	0.05	Smooth
7	3050	10	-	-
8	3500	10	0.05	Rough(1.3mm)
9	1900	10	0.05	Rough(1.3mm)
10	3800	10	0.05	Rough(5.0mm)

seems to be the same except that at the entrance smaller slope is observed for the case where the plate is at mid depth.

Experiment run #7 was conducted as an open channel flow with 50mm depth. The difference with run #5 and run#6 is that the approach flow is halved. Comparison between the two set-ups was necessary to check as how far the deposition is affected by a presence of a plate. Fig. 8.3 gives the plotting for both the cases. It is indicated that the peak deposition is slightly higher for the open channel flow, otherwise the deposition patterns seem to be similar.

The comparison of deposition between a smooth and rough top boundary is given by Fig. 8.4. Run #9 for rough boundary indicates a shift of the peak deposition. Otherwise comparing the results, at average there is no significant difference in the deposition pattern. It was not possible to repeat the same experiment and obtain exactly the same result. Hence the shift in the peak could be taken as an indication of the statistical variation from the average value.

The last experiment was conducted to study the effect of roughness size on the sediment deposition property. Fig. 8.5 shows the sediment deposition pattern for two

different types of roughness selected. Run #8 and run #9 were made for roughness size of 1.3mm and run #10 was made for roughness size of 5mm. The figure indicates a lower peak deposition for the more rough top boundary. But the removal ratio is not significantly different for each types of roughness considered.

8.1 Computational result

To study the sediment deposition pattern using a numerical computation, it was necessary to define the flow variables. The TEACH code as discussed in chapter 6 is used to obtain computational results for velocity and momentum transfer coefficient profiles. The results are given by Fig. 8.6 for flow between smooth parallel plates. The profiles for flow between a rough and a smooth plate are given by Fig. 8.7. Considering the momentum transfer coefficient profile for flow between smooth parallel plates, it can be seen that at the central middle third of the flow its value almost constant and at maximum, as discussed in the theoretical background. This confirms the discussion given by Ismail('52). As it would be expected for the rough and smooth surface boundary the profiles are not symmetrical. The velocity profile near the rough surface is steeper due to the high shear stress generated by the roughness element. The momentum transfer coefficient is also higher for the same reason.

The numerical computational result for sediment deposition pattern is given by Fig. 8.8. As it is shown in the figure, no significant difference in deposition pattern is indicated between the smooth-smooth and rough-smooth flow. This is in accordance with the experimental observation.

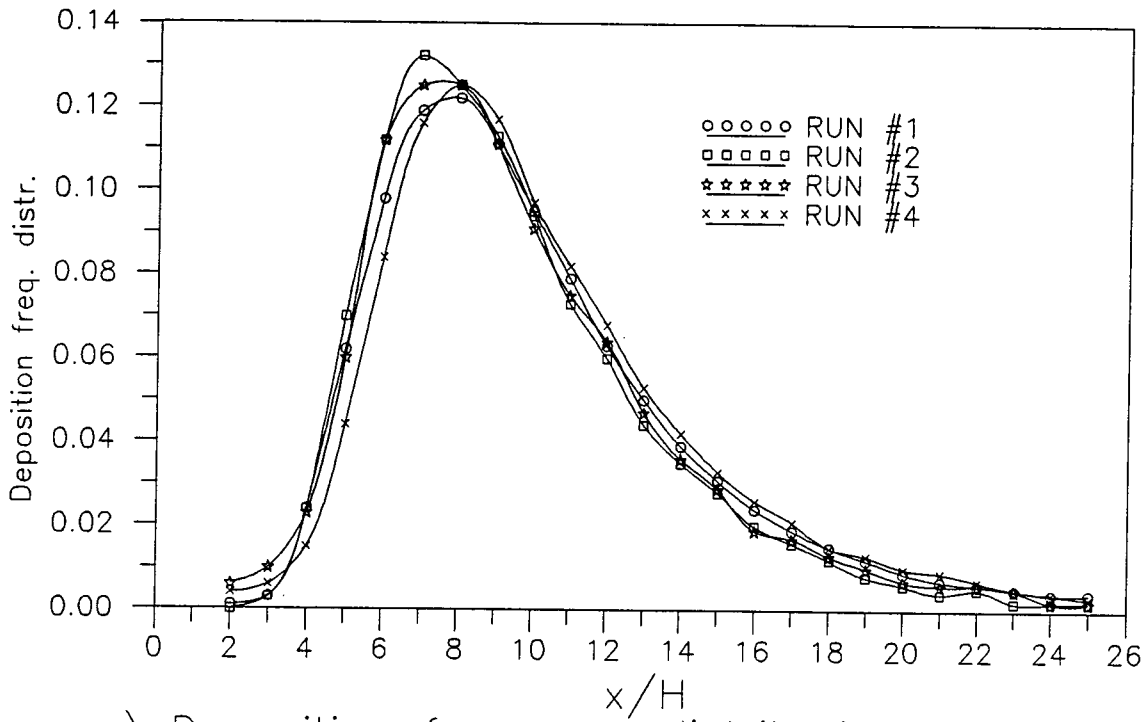

a) Deposition frequency distribution.

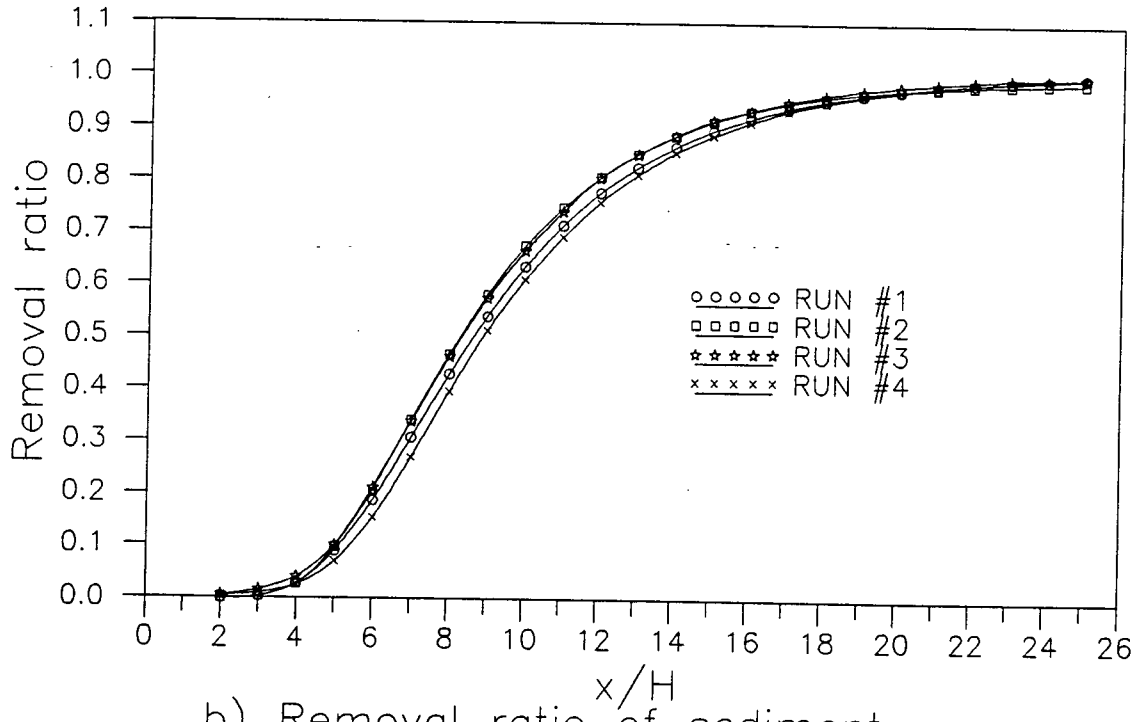

b) Removal ratio of sediment.

Figure 8.1: Deposition for free surface(100mm) and smooth plate

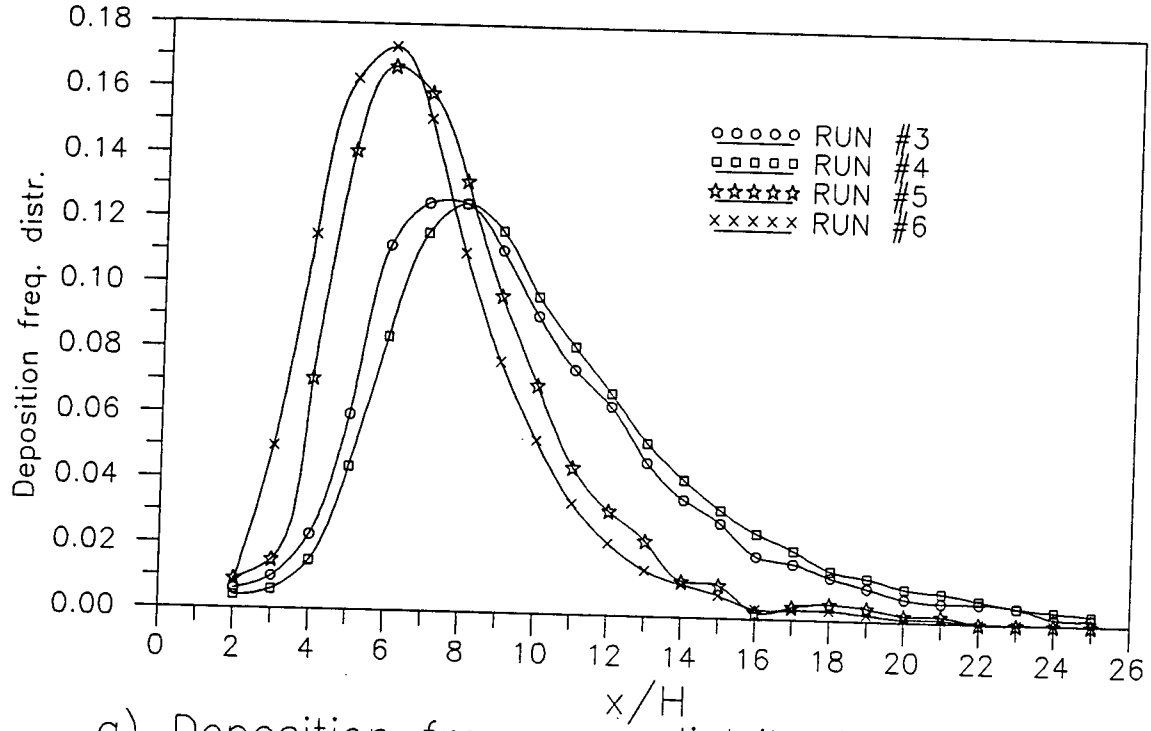

a) Deposition frequency distribution.

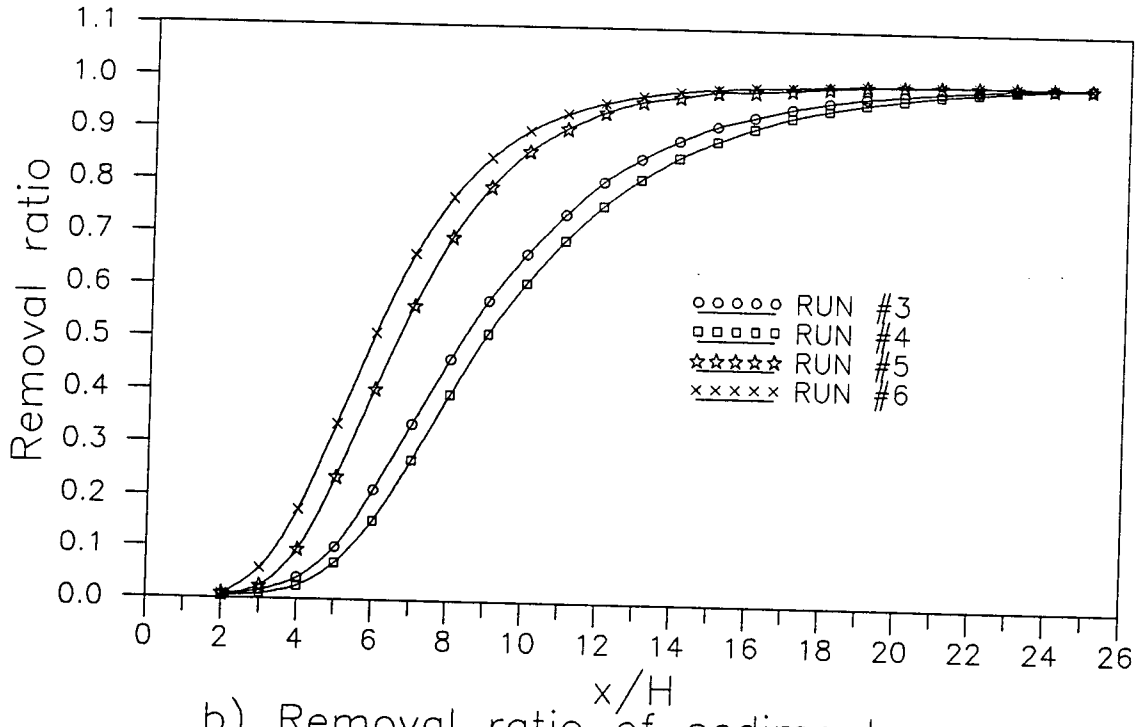

b) Removal ratio of sediment.

Figure 8.2: Deposition for free surface(100mm) and plate at mid depth

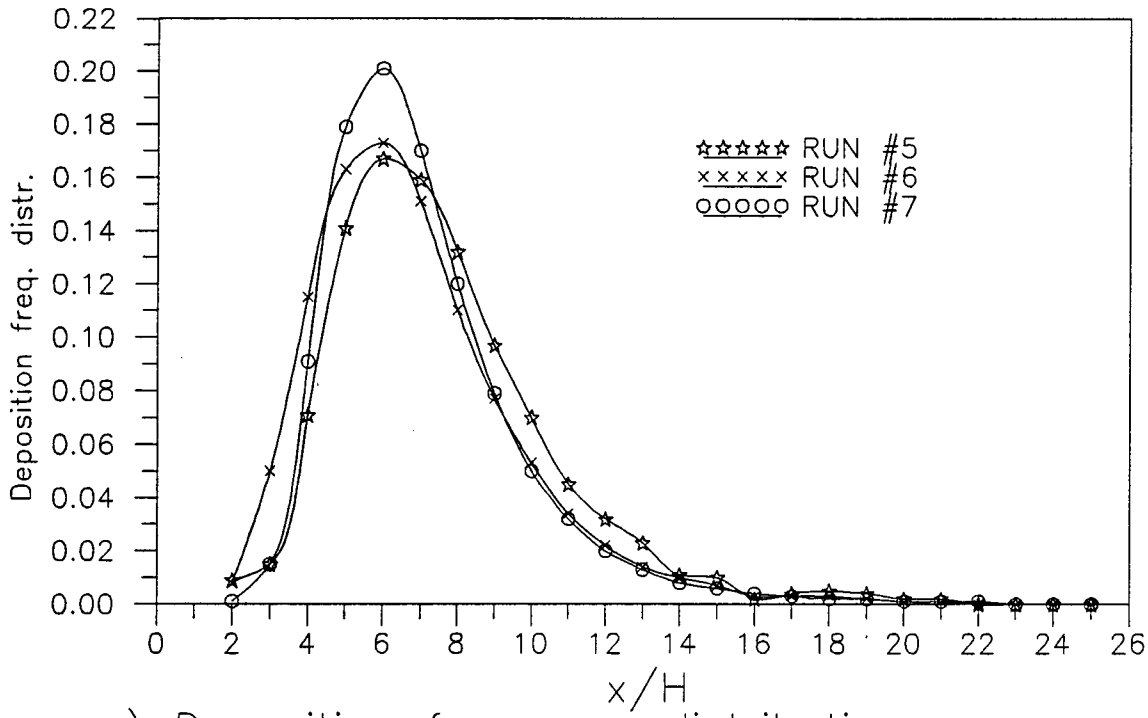

a) Deposition frequency distribution.

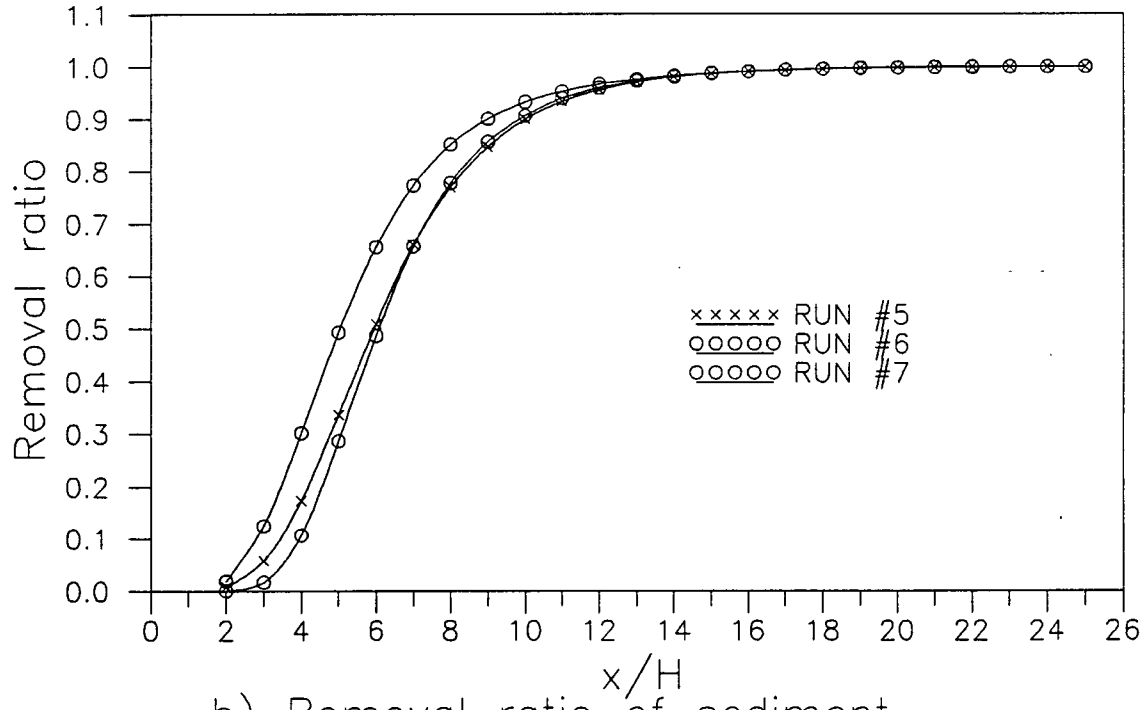

b) Removal ratio of sediment.

Figure 8.3: Deposition for free surface (50mm) and plate at mid depth

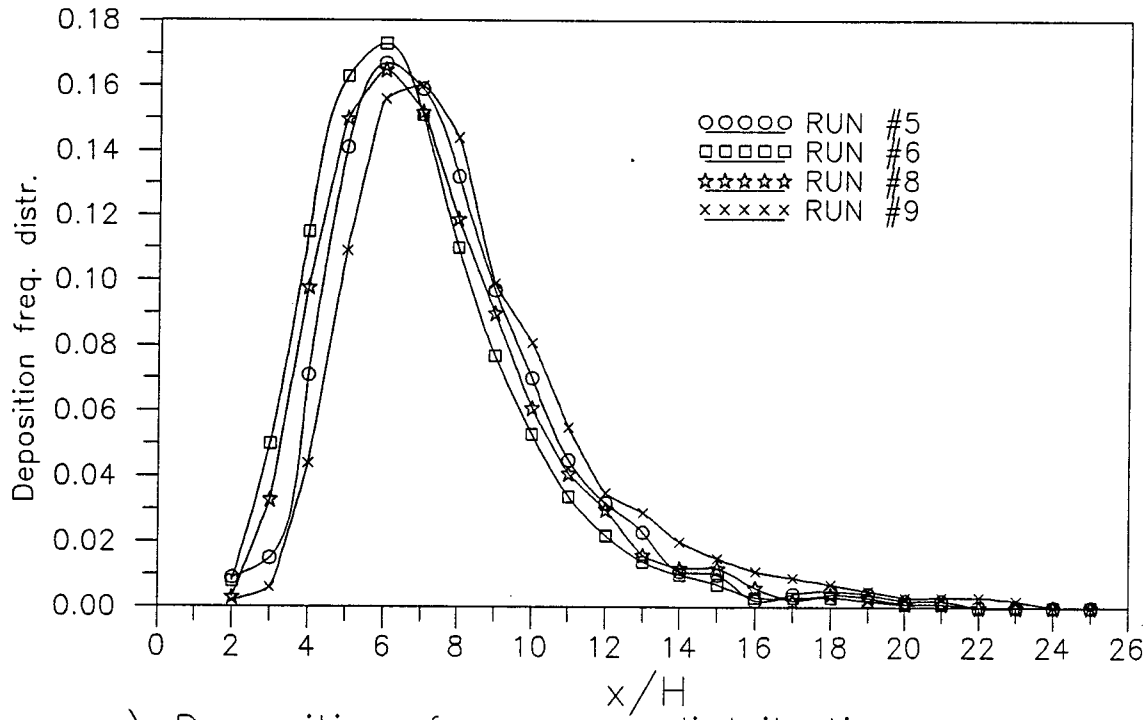

a) Deposition frequency distribution.

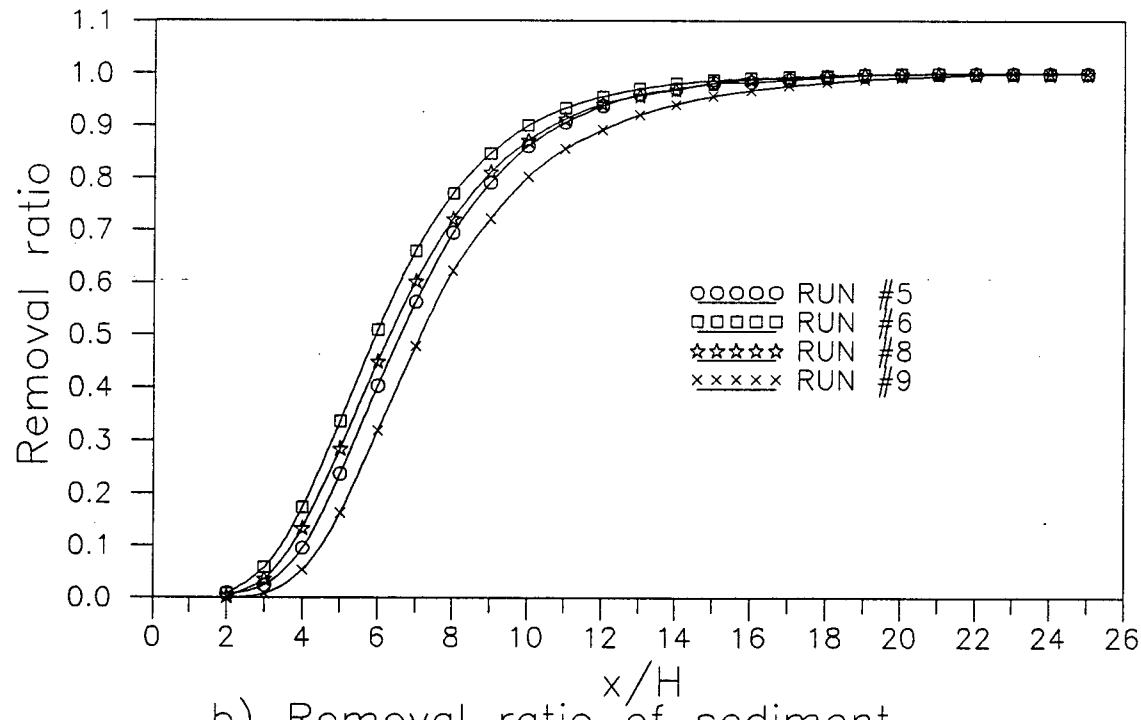

b) Removal ratio of sediment.

Figure 8.4: Deposition for smooth and rough plates

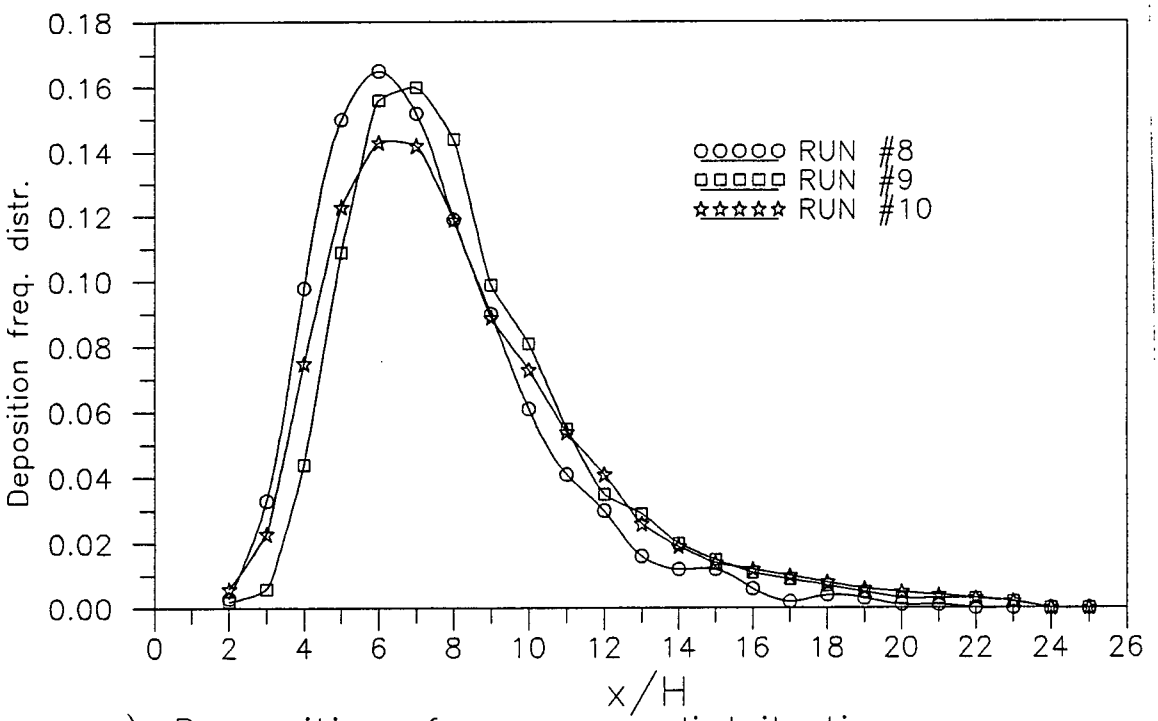

a) Deposition frequency distribution.

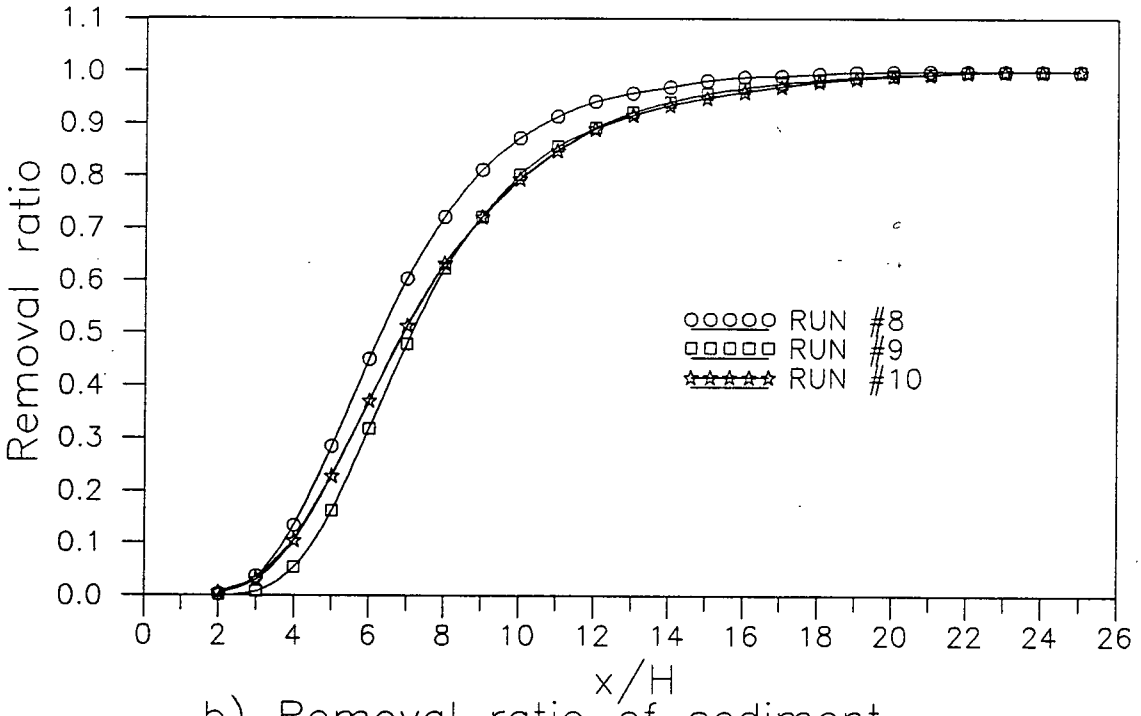

b) Removal ratio of sediment.

Figure 8.5: Deposition for different roughness plates

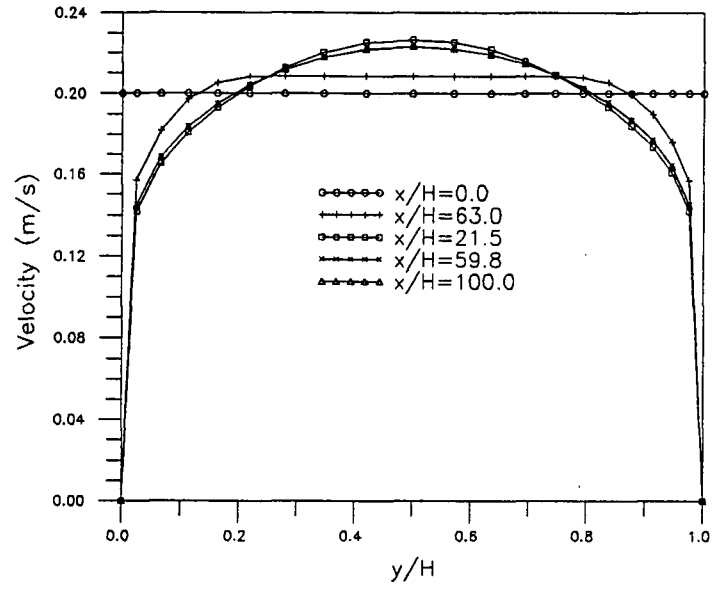

a) Velocity profile

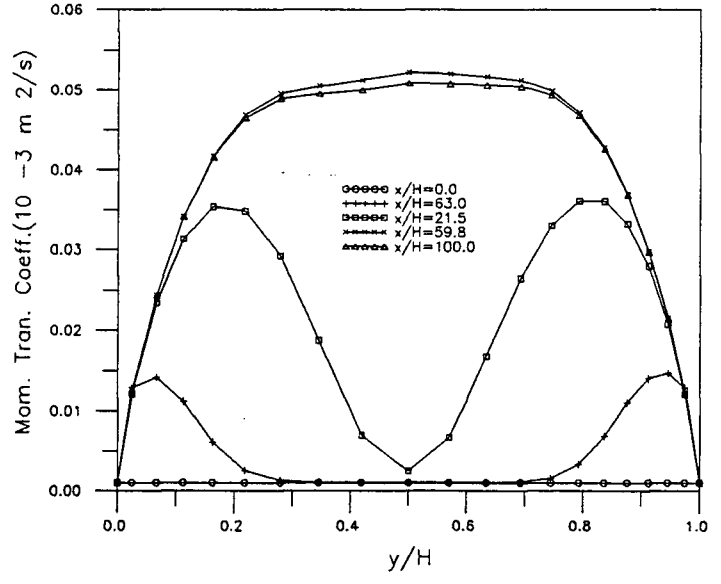

b) Mom. Tran. Coeff. profile

Figure 8.6: Flow between parallel plates

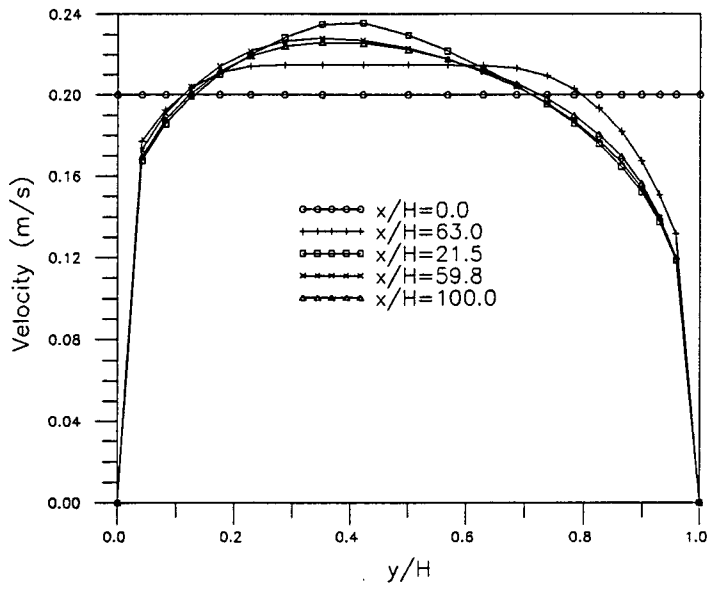

a) Velocity profile

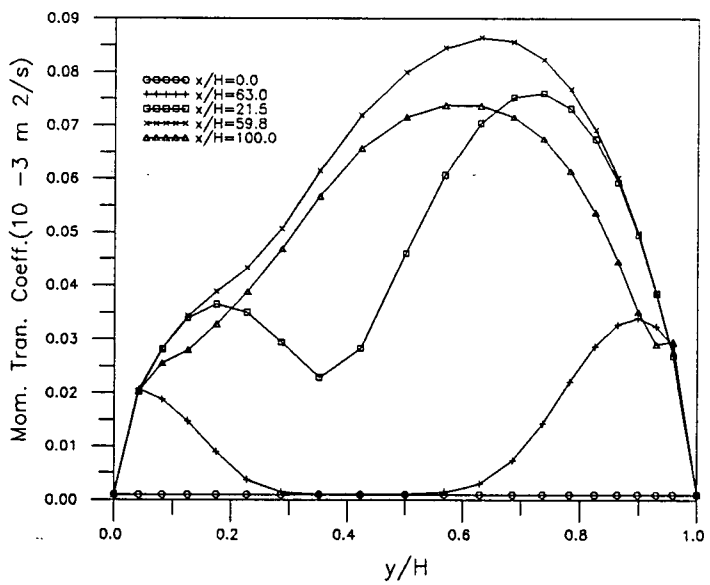

b) Mom. Tran. Coeff. profile

Figure 8.7: Flow between rough and smooth plate

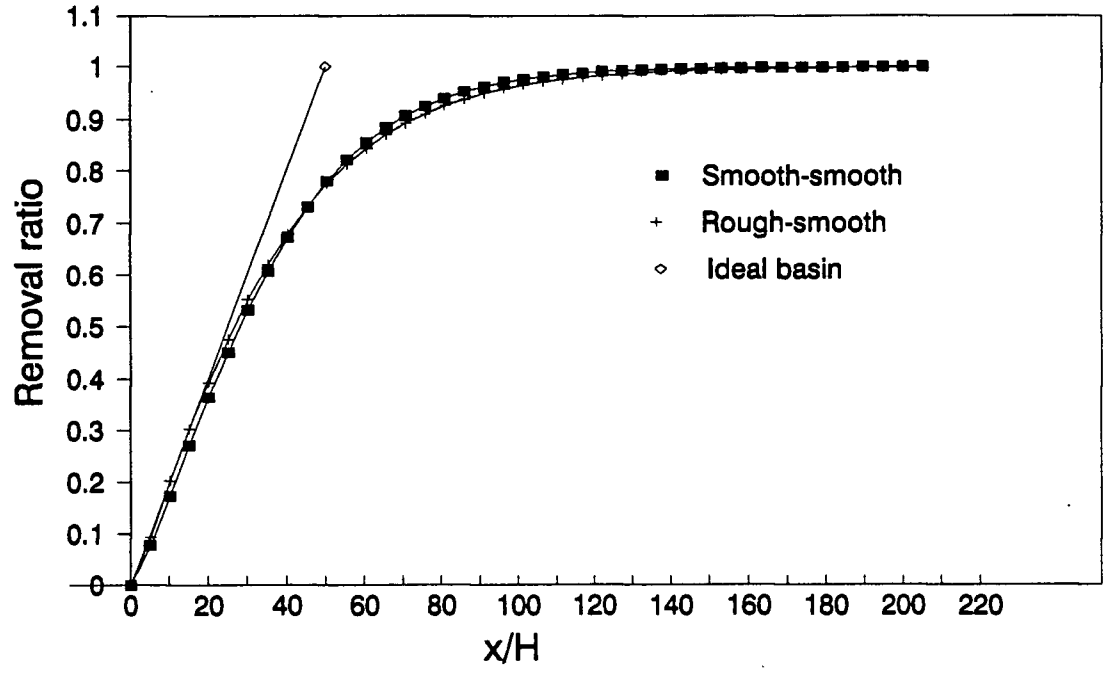

a) Removal ratio of sediment.

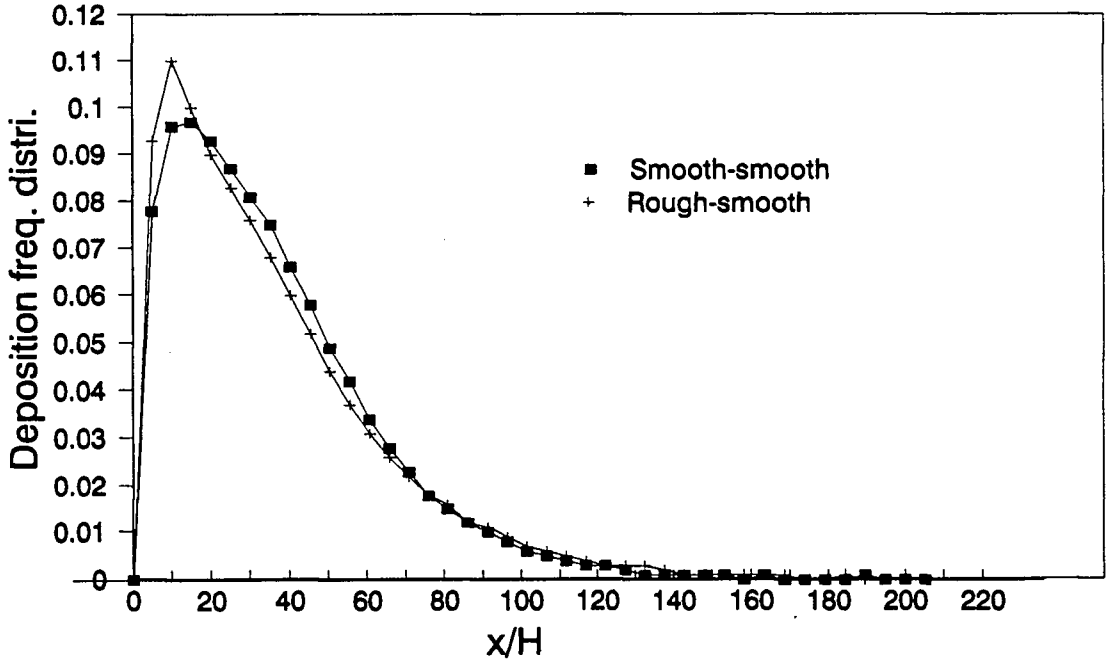

b) Deposition frequency distribution.

Figure 8.8: Numerical result for sediment deposition

Chapter 9

CONCLUSIONS

The total investigation consists of two sets of experiments and a theoretical numerical calculation of sedimentation. One set of experiments studied a settling tank for a fish rearing system and took into account all the constraints imposed by the rest of the system. A further set of experiments examined a more idealized arrangement of just one component of the total system. This arrangement was also analyzed theoretically.

The first set of experiments was carried out to investigate the effectiveness of using a stack of horizontal plates to increase sediment removal from a flow. This first set of experiments investigated a complete settling system for a fish rearing system and is reported in Chapter 4. These experiments confirmed that it is possible to use a stack of horizontal parallel plates to make maximum use of a limited space available in a settling tank. The efficiency of the settling tank was highly dependent on the flow distribution among the settling plates and it was found that circulation of flow within the tank has to be avoided since it has a big influence on the performance. The sediment deposition pattern between the settling plates contributes to the overall efficiency of the settling tank. Practical considerations at the entrance to the settling basin gave a concentrated high speed turbulent flow which disrupted the sedimentation process. To achieve a more uniform distribution of flow between each set of plates and to prevent a general circulation of flow within the settling chamber, it was necessary to design a set of deflecting plates at tank inlet. These deflecting plates were arranged at different levels at the inlet to deflect the incoming high velocity vertical flow horizontally at various levels of the tank

at the inlet section. The dimensions and positions of the deflecting plates for maximum efficiency were determined experimentally. The resulting geometrical design is given by Fig. 4.4 and Fig. 4.5 in Chapter 4.

In a second set of experiments an idealized simple system was studied to find a way of improving the settling efficiency of a sedimentation basin. Bagnold('66) explains that sediments are kept in suspension due to anisotropic turbulence in the vertical direction produced near a bed surface. If the argument put forward by Bagnold('66) and supported by work of Irmay('80) suggests that the shear near a bottom boundary induces an upward supporting stress which supports sediment in suspension, then it was argued that a plate at the upper boundary would cause a downward turbulent stress, which should increase deposition of sediment. This argument was investigated by designing suitable experimental set-up as indicated in Chapter 7. The three different cases considered in the experiments are a) open channel flow, b) flow with upper smooth boundary and c) flow with upper rough boundary. The sediment was injected at the same position in each case and the deposition pattern observed. This was necessary to investigate a) the effect of upper boundary on sedimentation, b) the effect of positioning a horizontal plate in a flow on the settling of sediment and c) the effect of rough upper boundary on sedimentation.

Clearly, introducing extra plates, in a multiplate sedimentation, will increase sedimentation because it is equivalent to having a much larger settling basin. One set of experiments, Fig. 8.2, showed an increase in sedimentation when a plate was placed at mid-level of the flow. The reason for this increase are still not clear, because there are several factors to be considered. For example, in the tests reported in Fig. 8.2, the approach flow turbulence and velocity distribution were similar, but the introduction of a plate at half depth will tend to reduce the scale of the approach flow turbulence. Also a boundary layer will develop on the upper plates and the turbulence in this boundary layer will influence more of the cross-section as the boundary layer thickens.

In a second experiment, Fig. 8.1, free surface flow of a given depth was compared with flow with a top plate, but of the same water depth. This test showed no significant change in sedimentation rate. This result may be explained because the upper boundary layer takes time to develop and therefore the flow with the plate is probably very similar to the free surface case. Therefore there is still an interesting difference between the results of these two experiments, Fig. 8.1 and Fig. 8.2, one which indicates a significant improvement in settling rate and one which does not. This clearly needs further work.

The further series of tests used a rough upper plate to test whether this would increase settling rate, but no benefit was found. This was also indicated by the numerical result obtained. The reason for no increase in settling could be that at the inlet section the shear stress produced due to flow transition from free surface to solid boundary is so high that it exceeds the effect of providing roughness.

The comparison between a flow with a plate positioned at mid depth and that of free surface flow with half approach depth of the previous shows that the latter has slightly higher peak deposition. The approach depth of flow for each case is different and hence the ambient turbulence level at the inlet. This may be one of the reasons for the difference observed in the deposition pattern. Flow depth of a free surface flow seems to have an effect on the sediment deposition pattern. This can be explained by the difference of turbulence level generated in different flow depths due to different Reynolds numbers.

This flow between parallel plates is fairly similar to closed conduit flow. For high flows, sediment transport exists in closed conduits. This indicates the existence of net upward turbulent stress produced between the upper and lower boundary. From published measurements (for example Graf('71) and Ismail('52)) it can be seen from the velocity profile that the shear stress at the top and bottom walls is not the same. Since the bottom boundary experiences a higher shear stress than the upper boundary a net upward momentum flux is created to keep sediments in suspension.

Bibliography

[1] Abdel-Gawad, S. M., and McCorquodale, J. A., "Numerical Simulation of Rectangular Settling Tanks," *Journal of Hydraulic Research,* Vol. 23, No. 2, 1985, pp. 85-100.

[2] Bagnold, R. A., "An Approach to the Sediment Transport Problem from General Physics," *U.S. Geological Survey Professional Paper*, 422-I, 1966.

[3] Bayazit, M., "Turbulent Transfer Characteristics of Settling Phenomenon," *Proceedings of the 14th Congress of the IAHR,* Vol. 1, 1971.

[4] Bechteler, W., and Schrimpf, W., "Improved Numerical Model for Sedimentation," *Journal of Hydraulic Engineering,* Vol. 110, No. HY3, March, 1984, pp. 234-246.

[5] Blinco, P. H., and Partheniades, E., "Turbulence Characteristics in Free Surface Flows over Rough and Smooth Boundaries," *Journal of Hydraulic Research,* 9, 43, 1972, 43-69.

[6] Camp, T. R., "Sedimentation and the Design of Settling Tanks," *Transactions,* ASCE, Paper No. 2285, Vol. 111, 1946, pp.895-958.

[7] Çeçen, K., "Hydraulic Criteria of Settling Basins for Water Treatment, Hydropower and Irrigation," *Proceedings of the 17th Congress of the IAHR,* Vol. 4, 1977.

[8] Çeçen, K., and Sümer, M., "Longitudinal Distribution of Matters Settling to the Bed in Settling Basins," *Proceedings of the 14th Congress of the IAHR,* Vol. 1, 1971.

[9] Coleman, N. L., "Flume Studies of the Sediment Transfer Coefficient," *Water Resources Research,* Vol. 6, No. 3, June, 1970, pp. 801-809.

[10] Dobbins, W. E., "Effect of Turbulence on Sedimentation," *Transactions,* ASCE, Vol. 109, Paper No. 2218, 1944, pp. 629-656.

[11] Garde, R. J., and Ranga Raju, K. G.,*Mechanics of Sediment Transportation and Alluvial Stream Problems,* 2nd ed., Wiley Eastern Limited, 1985.

[12] Graf, W. H., *Hydraulics of Sediment Transport,* 1st ed., McGraw-Hill Book Co., Inc., New York, 1971.

[13] Gosman, A. D., and Ideriah, F.J.K., "TEACH T: A General Computer Program for Two Dimensional, Turbulent, Recirculating Flows," Report, Department of Mechanical Engineering, Imperial College, London, U.K., 1976.

[14] Hama, F. R., "Boundary-Layer Characteristics for Smooth and Rough Surfaces," Transactions of the Society of Naval Architecture and Marine Engineers, Vol. 62, 1954, pp. 333-358.

[15] Hazen, A., "On Sedimentations," *Transactions,* ASCE, Vol. 53, Paper No. 980, Dec., 1904, pp. 45-88.

[16] Hinze, J. O., *Turbulence,* McGraw-Hill Book Co., Inc., New York, 1959.

[17] Hippola, U. T. B., "Influence of Suspended Sediment Distribution on Settling Basin Design," *International Symposium on River Mechanics, IAHR,* Bangkok, Thailand, Jan., 1973 pp. 277-288

[18] Irmay, S., "Accelerations and Mean Trajectories in Turbulent Channel Flow," *Transactions,* ASCE, Dec., 1980.

[19] Ismail, H. M., "Turbulent Transfer Mechanism and Suspended Sediment in Closed Channels," *Transactions,* ASCE, Vol. 117, 1952, pp.409.

[20] Jobson, H. E., and Sayre, W. W., "Vertical Transfer in Open Channel Flow," *Journal of the Hydraulics Division,* ASCE, Vol. 96, No. HY3, Mar., 1970, pp. 703-724.

[21] Jobson, H. E., and Sayre, W. W., "Predicting Concentration Profiles in Open Channels," *Journal of the Hydraulics Division,* ASCE, Vol. 96, No. HY10, Oct., 1970, pp. 1983-1996.

[22] Kolmogorov, A. N., "Equations of Turbulent Motion in an Incompressible Fluid," *Izv. Akad. Wauk. SSSR, Sexia fizicheska,* VI, 1-2, 56-58, 1968.

[23] Larsen, P., Rissler, S., "On the Hydraulics of Settling Basin Inlets," *Proceedings of the 17th Congress of the IAHR,* Vol. 4, 1977, pp. 309-316.

[24] Laufer, J., "The Structure of Turbulence in Fully Developed Pipe Flow," *Report 1174,* National Advisory Committee for Aeronautics, 1954.

[25] Laufer, J., "Investigation of Turbulent Flow in a Two-Dimensional Channel," *Report 1053,* National Advisory Committee for Aeronautics, 1951.

[26] Launder, B. E., and Spalding, D. B., "The Numerical Computation of Turbulent Flows," *Computer Methods in Applied Mechanics and Engineering,* Vol. 3, North-Holland Publishing Co., 1974, pp. 269-289.

[27] Mashauri, D. A., *Modelling of a Vortex Settling Basin for Primary Clarification of Water,* Tempere University of Technology, Pub. 42, Tempere, 1986.

[28] Masonyi, E., *Water Power Development,* Vol. 2, 2nd ed., Academia Kiado, Budapest, Hungary, 1965.

[29] McQuivey, R. S., Richardson, E. V., "Some Turbulence Measurement in Open Channel Flow," *Journal of the Hydraulics Division,* Vol. 95, No. HY1, Jan., 1969, pp. 209-223.

[30] Patankar, S. V., *Numerical Heat Transfer and Fluid Flow,* Hemisphere Publishing Corporation, New York, 1980.

[31] Perry, A. E., "Rough Walls Boundary Layers," *Journal of Fluid Mechanics,* 37, 1969, pp. 383-413.

[32] Perry, A. E., Schofield W. H., Joubert, P. N., "Rough Wall Turbulent Boundary Layers," *Journal of Fluid Mechanics,* Vol. 37, Part 2, 1969, pp. 383-503.

[33] Prandtl, L., "Uber ein neues Formel-System fur die ausgenbildate Turbulenz," *Nacr. Akad. Wiss.* Gottingin, Math.-Phys., K.L., 6, 1945.

[34] Prandtl, L., *Essentials of Fluid Dynamics,* London, Blakie and Son, 1952.

[35] Richardson E. V., and McQuivey, R. S., "Measurement of Turbulence in Water," *Journal of the Hydraulics Division,* Vol. 94, No. HY 2, Mar., 1968, pp. 411-429.

[36] Rodi, W. "Turbulent Models and their Applications to Hydraulics, A State of the Art Review," IAHR, Delft, The Netherlands, 1984.

[37] Sarikaya, H. Z., "Numerical Model for Discrete Settling," *Journal of the Hydraulics Division,* ASCE, Vol. 103, No. HY8, Aug., 1977, pp. 865-876.

[38] Schamber, D. R., and Larock, B. E., "Numerical Analysis of Flow in Sedimentation Basins," *Journal of the Hydraulic Division,* ASCE, Vol. 107, No. HY5, May, 1981, pp. 575-591.

[39] Schlicting, H., *Theory of Boundary Layers,*6th ed., McGraw-Hill Book Co. Inc. New York, 1968.

[40] Shaubauer, G. B., "Turbulent Process as Observed in Boundary Layer and Pipe," *Journal of Applied Physics,* Vol. 25, No. 2, 1954, pp. 188.

[41] Strand, R. I., "Sedimentation at Canal In-Line Structures," *Water Forum '86,* 1986, pp. 885-889.

[42] Takamatsu, T., Naito, M., Shiba, S., and Ueda, Y., "Effects of Deposit Resuspention on Settling Basin," *Journal of Environmental Engineering Division,* ASCE, Vol. 100, No. EE4, Aug., 1974, 883-903.

[43] Townsend, A.A., *The structure of Turbulent Shear Flow,* Cambridge University Press, 1956.

[44] Vanoni, V. A., "Transportation of Suspended Sediments by Water," *Transactions,* ASCE, Vol. 111, No.2267, 1946, pp. 67-133.

[45] Vanoni, V. A., Ed., *Sedimentation Engineering,* ASCE, Manuals and Reports on Engineering Practice, No. 54, 1975.

[46] Wilson, G. E., "Coupling Free Vortex Energy Dissipation with Sediment Control," *Water Forum '86,* 1986, pp. 421-426.

[47] Yao, K. M., "Design of High-Rate Settlers," *Journal of Environmental Engineering Division,* ASCE, Vol. 99, No. EE5, Oct., 1973, pp. 621-637.

Appendix A

Wall Function Treatment

The wall function treatment given by Launder and Spadling('74) has two assumptions: first, the flow near the wall is taken as Couette flow and secondly the turbulence characteristics near the wall are associated with the inertial sublayer.

Considering a grid point P adjacent to a wall, Fig. E.1, for the shear stress to be constant and equal to the wall shear stress, the point is assumed to be close to the wall. Defining the non-dimensional distance y^+ as

$$y^+ = U_* y_P / \nu \tag{A.1}$$

$$y^+ \leq 200 \tag{A.2}$$

Neglecting the negligible pressure gradients, the momentum equation reduces to

$$\frac{1}{\rho}(\mu + \mu_t)\frac{\partial U}{\partial y} = \frac{\tau}{\rho} \simeq \frac{\tau_w}{\rho} \tag{A.3}$$

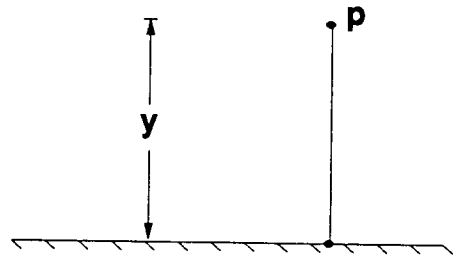

Figure A.9: Grid point near wall

Non-dimensionalizing the velocity as

$$U^+ = \frac{U}{U_*} \tag{A.4}$$

Eq. A.3 reduces to

$$\left(1 + \frac{\mu_t}{\mu}\right) \frac{dU^+}{dy^+} = 1 \tag{A.5}$$

The near wall region may be divided into viscous sublayer where molecular viscosity is dominant, and inertial sublayer where the turbulent viscosity term is dominant as given below

$$\frac{\mu_t}{\mu} \ll 1 \qquad y^+ < 11.63 \tag{A.6}$$

$$\frac{\mu_t}{\mu} \gg 1 \qquad y^+ \geq 11.63 \tag{A.7}$$

Integrating Eq. A.5 for $y^+ < 11.63$, viscous sublayer region,

$$U^+ = y^+ \tag{A.8}$$

A.1 Smooth Wall

For fully turbulent flow where $y^+ \geq 11.63$, from the mixing length concept, Hinze('59):

$$\mu_t = \kappa \rho U_* y \tag{A.9}$$

Substituting the above into Eq. A.5 and integrating

$$U^+ = \frac{1}{\kappa} ln(E y^+) \tag{A.10}$$

which is the logarithmic law of the wall, where E=9, is a constant of integration.

A.2 Rough Wall

A wall is said to be hydraulically rough or smooth depending on the size of roughness and flow characteristics. The non-dimensional roughness may be defined as

$$k_s^+ = \frac{U_\tau}{\nu} \tag{A.11}$$

where k_s is the equivalent sand roughness. For $k_s^+ > 50$ a wall is considered to be hydraulically rough, Townsend('56). Therefore Eq. A.10 is written as

$$U^+ = \frac{1}{\kappa} ln \left(E_1 \frac{y}{k_s} \right) \tag{A.12}$$

where the constant, $E_1 = 30$ for rough sand surfaces.

The TEACH code assumes a hydraulically smooth surface boundary. The above formulation was incorporated in the code to handle rough wall surfaces.

For rough surfaces the point of origin for the velocity distribution (Eq. A.12) is between the edge and base of the roughness element. According to the study and comparisons made by Perry et al.('69) and Blinco et al.('72), the origin is taken to be $0.25k_s$ from the edge to the base of the roughness considered. Accordingly the TEACH code was also modified.

Appendix B

TEACH Code Solution Procedure

1. All field varables are guessed.
2. The coefficient of momentum equations are assembled (after modifying for boundary conditions) to solve for velocities using prevailing pressures.
3. Coefficients and mass sources for pressure correction equations are calculated to solve for pressure corrections.
4. The pressures and velocities are updated according to the corrections calculated.
5. Other variables are solved after assembling the coefficients, with proper boundary condition treatment.
6. Convergence is tested. If not convergent, the prevailing fields are used as new guess and the procedure repeated from step 2.